MOX-Report No. 74/2024

A mixed-dimensional model for the electrostatic problem on coupled domains

Crippa, B., Scotti, A.; Villa, A

MOX, Dipartimento di Matematica
Politecnico di Milano, Via Bonardi 9 - 20133 Milano (Italy)

mox-dmat@polimi.it https://mox.polimi.it

A mixed-dimensional model for the electrostatic problem on coupled domains

Beatrice Crippa[1], Anna Scotti[1], Andrea Villa[2]

[1] MOX-Laboratory for Modeling and Scientific Computing, Department of Mathematics, Politecnico di Milano, 20133 Milan, Italy

[2] Ricerca Sul Sistema Energetico (RSE), 20134 Milano, Italy

Abstract. We derive a mixed-dimensional 3D-1D formulation of the electrostatic equation in two domains with different dielectric constants to compute, with an affordable computational cost, the electric field and potential in the relevant case of thin inclusions in a larger 3D domain. The numerical solution is obtained by Mixed Finite Elements for the 3D problem and Finite Elements on the 1D domain. We analyze some test cases with simple geometries to validate the proposed approach against analytical solutions, and perform comparisons with the fully resolved 3D problem. We treat the case where ramifications are present in the one-dimensional domain and show some results on the geometry of an electrical treeing, a ramified structure that propagates in insulators causing their failure.

1. Introduction. The aim of this work is to obtain a geometrically reduced formulation of the electrostatic equation on two coupled domains representing materials with different electrical properties, more specifically, a thin fracture inside a wide three-dimensional domain. In particular, we are interested in modelling the electric field and potential inside the electrical treeing [4, 12], which is a self-propagating defect, characterized by long and thin branches [36, 34], causing the deterioration of insulating components of electrical cables. The defect is filled with gas, with a dielectric constant close to 1, while the external material is typically a solid insulator with higher dielectric constant.

The inclusion of thin and ramified domains within wide three-dimensional volumes is a challenge common to many fields, such as the modeling of fluid flow in fractured porous media [27], microvascular blood flow [18] and drug delivery through microcirculation [13], besides defect propagation inside dielectric materials. The discretization of problems on such domains involves high computational complexity, due to difficulties in mesh generation and a large number of degrees of freedom. One common approach to reduce this complexity consists in the approximation of the intricate inner domain as a one-dimensional domain, thereby reducing it to its skeleton [16, 31, 14]. This approximation allows to overcome the difficulty of generating a fine three-dimensional mesh on the inner thin domain and to consider a coarser mesh on the external domain as well. Notaro *et al.* [30] proposed a mixed Finite Element Method (FEM) for the solution of coupled problems in 3D and 1D domains, extending the idea of D'Angelo [15] for three-dimensional problems involving line sources. The presence of a line source still represents a challenge due to the singularity of the solution, as discussed in [22], where a singularity removal method is proposed. For a more accurate numerical solution around the 1D domain on coarser meshes, Extended Finite Elements (XFEM) can be applied, as done in Březina and Exner [9], Gracie and Craig [24] and [25] for 3D problems with 1D source, and coupled mixed-dimensional coupled problems.

In this work we will reduce the treeing domain to a one-dimensional graph, adapt the full model introduced by Villa *et al.* [39] to a mixed-dimensional framework and numerically solve it

This work has been financed by the Research Found for the Italian Electrical System under the Contract Agreement between RSE and the Ministry of Economic Development.

with the Finite Element Methods. The reduction of this problem presents some criticalities related to the profile of the electric potential in the gas domain, with a non-negligible dependence on the radial coordinate, and the presence of a jump in the normal component of the electric field across the interface between the two materials. We propose a dual-primal formulation of the problem, modelling the evolution of both electric field and potential in the solid 3D domain and only the potential in the 1D domain, where the electric field can be computed a posteriori, keeping into account also its components non-tangential to the 1D domain. To account for the dependence of the potential in the gas on the radial coordinate we rely on the knowledge of the potential profile associated with a constant, given charge distribution.

Let us review the structure of the paper. In Section 2 we present the model equation and describe the equidimensional domains in the simple case where the inner one does not present branches. We then derive the mixed-dimensional formulation in Section 3 and establish its well-posedness in Section 4. We extend the model to also account for branches and bifurcations in Section 5 and introduce the numerical methods for the solution of the complete problem in Section 6. Finally, we present three test cases in Section 7: the validation of the proposed reduction is on a simple geometry with a single one-dimensional line as inner domain, the application of the model to a short line immersed in a cylindrical 3D domain, and finally to the intricate structure of an electrical treeing.

2. The 3D problem. To model the evolution of the electric field $\mathbf{E}$ and potential Φ on two domains filled with materials with different permittivities we consider the electrostatic equation [26]. The problem is defined on a three-dimensional domain Ω, such as the one represented in Figure 1, composed of a subdomain Ω_g, assumed cylindrical, typically filled with gas, surrounded by a solid insulator Ω_s. We call Λ the centerline of Ω_g, defined as $\Omega_g = \{\mathbf{x} \ : \ \text{dist}(\mathbf{x}, \Lambda) \leq R\}$. This inner domain represents a branch of the electrical treeing, which will be thoroughly treated in the next sections. We suppose that in Ω_s there is null electric charge, while in the gas the charge density is given by a function $q \ : \ \Omega_g \to \mathbb{R}$. Let us introduce the coefficient $\epsilon : \ \Omega \to \mathbb{R}$, modeling the dielectric constants taking values ϵ_s and ϵ_g in the two domains:

$$\epsilon = \begin{cases} \epsilon_s, & \text{in } \Omega_s, \\ \epsilon_g, & \text{in } \Omega_g, \end{cases}$$

and consider as unknowns of our problem the displacement field $\mathbf{D} = \epsilon\mathbf{E}$ and the potential Φ. We call $\mathbf{D}_s$, Φ_s and $\mathbf{D}_g$, Φ_g their restrictions to Ω_s and Ω_g, respectively. Then, the system of equations we will consider is the following:

$$\begin{cases} \nabla \cdot \mathbf{D}_g = \dfrac{q}{\epsilon_0}, & \text{in } \Omega_g, \\ \nabla \cdot \mathbf{D}_s = 0, & \text{in } \Omega_s, \\ \mathbf{D} = -\epsilon \nabla \Phi, & \text{in } \Omega. \end{cases} \tag{2.1}$$

We complete the problem with Neumann and Dirichlet boundary conditions on portions $\partial\Omega_D$ and $\partial\Omega_N$ of the boundary $\partial\Omega$, such that $\partial\Omega_D \cap \partial\Omega_N = \emptyset$ and $\partial\Omega_D \cup \partial\Omega_N = \partial\Omega$:

$$\begin{cases} \mathbf{D} \cdot \mathbf{n} = \nu, & \text{on } \partial\Omega_N, \\ \Phi = \Phi^b, & \text{on } \partial\Omega_D, \end{cases} \tag{2.2}$$

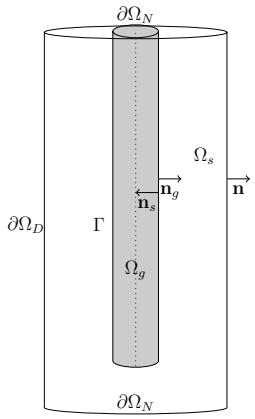

Figure 1. Domain Ω, given by a cylinder corresponding to the gas subdomain Ω_g, surrounded by a generic volume Ω_s, representing the dielectric domain.

where $\nu : \partial\Omega_D \to \mathbb{R}$ and $\Phi^b : \partial\Omega_N \to \mathbb{R}$ are the known Neumann and Dirichlet terms, respectively. The Neumann condition sets the value of the normal component of the displacement field $\mathbf{D}$ on the boundary $\partial\Omega_N$, while the Dirichlet condition fixes the value of the potential Φ on the boundary $\partial\Omega_D$.

Finally, we impose interface conditions on the surface $\Sigma = \{\mathbf{x} : \text{dist}(\mathbf{x}, \Lambda) = R\}$ separating the two domains. In particular, we consider a simplification of the system proposed in [40] where the displacement field presents a jump in the normal component, proportional to the total surface charge q_Γ and the potential is continuous:

$$\begin{cases} \mathbf{D}_s \cdot \mathbf{n}_s + \mathbf{D}_g \cdot \mathbf{n}_g = -\dfrac{e}{\epsilon_0} q_\Gamma, & \text{on } \Sigma, \quad (2.3a) \\ \Phi_s = \Phi_g, & \text{on } \Sigma. \quad (2.3b) \end{cases}$$

For the sake of simplicity, we start by considering two coaxial cylindrical domains Ω_g and Ω_s, as in Figure 1. We introduce a parametrization on the centerline Λ of Ω_g, so that we can define the coordinate $s \in [0, S]$ along it. In the following, we will assume that, if one endpoint of Λ belongs to the external boundary $\partial\Omega$ and the other one is internal to the solid domain Ω_s, the first one coincides with the point of coordinate $s = 0$ and the second with $s = S$. For every point $\mathbf{x}_s \in \Lambda$, having coordinate $s \in [0, S]$, we define the transversal section of Ω_g, orthogonal to the centerline, as $\mathcal{D}(s) = \{\mathbf{x} \in \Omega_g : |\mathbf{x} - \mathbf{x}_s| \leq R \text{ and } (\mathbf{x} - \mathbf{x}_s) \perp \Lambda\}$. In particular, we will denote the basis of the cylinder Ω_g immersed in the solid domain by $\mathcal{D}(S)$, while the one belonging to the external boundary of Ω by $\mathcal{D}(0)$. Moreover, we call $\Gamma = \bigcup_{s\in[0,S]} \partial\mathcal{D}(s)$ the lateral surface of Ω_g, so that the separating interface between the two domains in Figure 1 is $\Sigma = \Gamma \cup \mathcal{D}(S)$.

If we assume that the inner cylinder is very thin, i.e. its radius in much smaller than its length, we can approximate the coupled problem described above as a mixed-dimensional one, where Ω_g is collapsed on its one-dimensional centerline Λ and Ω_s is identified with the whole three-dimensional domain Ω. Another simplification we introduce is the assumption that the charge q is constant over sections of Ω_g, orthogonal to the axis of the cylinder, more precisely:

Assumption 1. *The gas domain is a cylinder with radius R and length L, with $R \ll L$.*

Assumption 2. *The total charge q in Ω is constant over sections $\mathcal{D}(s)$ orthogonal to its centerline Λ, $\forall s \in \Lambda$.*

In order to perform this dimensional reduction we start by separating the problems on the two domains, considering as unknowns the restrictions of the electric field and potentials on Ω_s and Ω_g. At this stage the boundaries becomes the unions of the external boundaries of each domain and the separating surface:

$$\partial\Omega_s = (\bar{\Omega}_s \cap \partial\Omega) \cup \Sigma;$$
$$\partial\Omega_g = (\bar{\Omega}_g \cap \partial\Omega) \cup \Sigma.$$

The interface conditions on Σ become boundary conditions for the two problems in this framework. We can separate the problems on the two domains, coupled by the interface conditions (2.3a)-(2.3b), and express the problem in the gas domain in primal form:

Find $\mathbf{D}_s \,:\, \Omega_s \to \mathbb{R}^3,\ \Phi_s \,:\, \Omega_s \to \mathbb{R},\ \Phi_g \,:\, \Omega_g \to \mathbb{R}$ such that

$$\begin{cases} \mathbf{D}_s + \epsilon_s \nabla \Phi_s = 0, & \text{in } \Omega_s, \quad (2.4a) \\ \nabla \cdot \mathbf{D}_s = 0, & \text{in } \Omega_s, \quad (2.4b) \\ \Phi_s = \Phi_g, & \text{on } \Sigma, \quad (2.4c) \\ \mathbf{D}_s \cdot \mathbf{n}_s = -\mathbf{D}_g \cdot \mathbf{n}_g + g, & \text{on } \Sigma, \quad (2.4d) \\ \Phi_s = \bar{\Phi}_s, & \text{on } \partial\Omega_{s,D}, \quad (2.4e) \\ \mathbf{D}_s \cdot \mathbf{n} = \nu_s, & \text{on } \partial\Omega_{s,N}, \quad (2.4f) \end{cases} \qquad \begin{cases} -\nabla \cdot (\epsilon_g \nabla \Phi_g) = f, & \text{in } \Omega_g, \quad (2.5a) \\ \Phi_g = \Phi_s, & \text{on } \Sigma, \quad (2.5b) \\ \epsilon_g \nabla \Phi_g \cdot \mathbf{n}_s = \mathbf{D}_s \cdot \mathbf{n}_g - g, & \text{on } \Sigma, \quad (2.5c) \\ \Phi_g = \bar{\Phi}_g, & \text{on } \partial\Omega_{g,D}, \quad (2.5d) \\ \nabla \Phi_g \cdot \mathbf{n} = \nu_g, & \text{on } \partial\Omega_{g,N}, \quad (2.5e) \end{cases}$$

where $f = \dfrac{q}{\epsilon_0}$, $g = -\dfrac{e}{\epsilon_0} q_\Gamma$, $\bar{\Phi}_s = \Phi\big|_{\partial\Omega_{s,D}}$, $\bar{\Phi}_g = \Phi\big|_{\partial\Omega_{g,D}}$, $\nu_s = \nu\big|_{\partial\Omega_{s,N}}$ and $\nu_g = -\nu\big|_{\partial\Omega_{g,N}}$.
In the following, we will perform the dimensionality reduction by integrating the first equation (2.5a) by parts, where the Neumann boundary conditions naturally appear, following the approach of Cerroni *et al.* [14]. This implies that the electric field in the gas domain is not directly computed as an unknown of our problem, but only as a postprocessing.

3. Model reduction. In this section we will derive the reduced mixed-dimensional model for the electric field and potential on two domains, modeled as coaxial cylinders, taking into account the interface conditions that prescribe continuity of the potentials and a jump discontinuity on the normal component of the displacement fields across Γ. This kind of geometrical reduction is typical of coupled problems describing flow models, with very similar sets of equations as (2.1). However, these models generally involve continuity of the scalar unknwon at the interface, as in equation (2.3b), but do not present a jump of the normal component of the vectorial unknown, unlike what we have in equation (2.3a) [25] [28]. As we will see in Section 3.2, another difference with respect to these works consists in the definition of the 1D variable, which is usually modeled as a constant, whereas in our case we are considering a splitting of Φ_g that allows us to model its radial variation.

3.1. ASSUMPTION ON THE POTENTIAL. We start by performing the reduction to one dimension of Ω_g and adapt the formulation of the problem in primal form in the gas domain (equations (2.5a)-(2.5e)). Therefore, we want to end up with an unknown electric potential which is only dependent on the coordinate s. However, the hypothesis of a constant potential on each section $\mathcal{D}(s)$, made

in the 1D reduction of problems in porous media, such as [14] [25] [28], is restrictive because, together with potential continuity at the interface, it would imply that the electric field has only one component, tangent to Λ. Moreover, the right-hand-side of equation (2.5a) represents the volume charge concentration, which was be assumed to be constant on sections (Assumption 2), and produces a non-negligible transversal electric field. As a consequence, the electric potential must be non-constant on sections.

The potential produced by a constant concentration of charge on each section can be analytically computed, thanks to Gauss theorem. We integrate the divergence of the electric field and charge concentration over a cylinder $\mathcal{W} \subseteq \Omega_g$, of radius $r \leq R$ and height h, considering h much smaller than the total length of Λ:

$$\int_{\mathcal{W}} \nabla \cdot (\mathbf{E}_g) = \int_{\mathcal{W}} \frac{q}{\epsilon_0}. \tag{3.1}$$

Thanks to Assumptions 1 and 2, and since, under the hypothesis of radially symmetric domain, the potential generated by uniform charge distribution has radial symmetry with respect to the center of the cylinder, the electric field line are orthogonal to the lateral surface $\mathcal{S}$ of $\mathcal{W}$. Then, the left hand side of equation (3.1) can be rewritten as:

$$\int_{\mathcal{W}} \nabla \cdot (\mathbf{E}_g) = \int_{\mathcal{S}} \mathbf{E}_g \cdot \mathbf{n}_g = -2\pi r \int_{s_1}^{s_2} \mathbf{E}_g(r,s) \cdot \mathbf{n}_g ds.$$

Then, equation (3.1) is equivalent to

$$-2\pi r \int_{s_1}^{s_2} \epsilon_g \nabla \Phi_g(r,s) \cdot \mathbf{n}_g ds = \pi r^2 \int_{s_1}^{s_2} \frac{q(s)}{\epsilon_0} ds, \quad \forall r \in (0,R],\ \forall s_1, s_2 \in \Lambda,$$

and therefore

$$\frac{\partial \Phi_g}{\partial r}(r,s) = -\frac{q(s)}{2\epsilon_0 \epsilon_g} r, \quad \forall r \in (0,R],\ \forall s \in \Lambda. \tag{3.2}$$

We finally integrate with respect to r and obtain the analytic expression of the potential in the gas domain:

$$\Phi_g(r,s) - \Phi_g(0,s) = -\int_0^r \frac{q(s)}{2\epsilon_0\epsilon_g} \rho d\rho = -\frac{q(s)}{2\epsilon_0\epsilon_g}\frac{r^2}{2} = -\frac{q(s)}{4\epsilon_0\epsilon_g} r^2, \quad \forall r \in (0,R],\ \forall s \in \Lambda. \tag{3.3}$$

Observe that the difference of potential on the left-hand side is continuous in the variable r and tends to vanish as r becomes smaller:

$$\lim_{r \to 0} (\Phi_g(r,s) - \Phi_g(0,s)) = 0.$$

Let us now define the following functions:

$$\Phi_\Lambda : \Lambda \to \mathbb{R}, \quad \Phi_\Lambda(s) = \Phi_g(0,s), \qquad \forall s \in \Lambda, \tag{3.4a}$$

$$\Phi_r : \Lambda \to \mathbb{R}, \quad \Phi_r(s) = -\frac{q(s)}{4\epsilon_0\epsilon_g}, \qquad \forall s \in \Lambda, \tag{3.4b}$$

$$\phi : [0,R] \to \mathbb{R}, \quad \phi(r) = r^2, \qquad \forall r \in [0,R]. \tag{3.4c}$$

Here, Φ_r and ϕ are known terms in the expression of Φ_g and take into account the radial effect of a constant charge distribution on sections, while the dependence on the longitudinal coordinate s is taken into account by the additive term Φ_Λ, which is constant over sections:

$$\Phi_g(s,r) = \Phi_\Lambda(s) + \Phi_r(s)\phi(r), \quad \forall r \in [0, R(s)],\ \forall s \in \Lambda, \tag{3.5}$$

By substituting this splitting of the potential in the interface conditions (2.5b)- (2.5c), we can now rewrite continuity of the potential and jump of the electric field on the lateral surface Γ as follows:

$$\Phi_r = \frac{\Phi_s - \Phi_\Lambda}{\phi(R)}, \qquad \text{on } \Gamma, \tag{3.6}$$

$$\mathbf{D}_s \cdot \mathbf{n}_s = g + \epsilon_g \nabla \Phi_g \cdot \mathbf{n}_g = g + \epsilon_g \nabla(\Phi_\Lambda(s) + \Phi_r(s)\phi(r)) \cdot \mathbf{n}_g = g + \epsilon_g \Phi_r \phi'(R), \quad \text{on } \Gamma,$$

and, combining them, we obtain a Robin interface condition:

$$\mathbf{D}_s \cdot \mathbf{n}_s = g + \epsilon_g \frac{\Phi_s - \Phi_\Lambda}{\phi(R)} \phi'(R), \qquad \text{on } \Gamma. \tag{3.7}$$

Observe that condition (3.6) implies that Φ_s on Γ can only depend on the coordinate s, which means that the trace $\hat{\Phi}_s$ of Φ_s on Γ can be approximated as a constant on the boundary of each section $\mathcal{D}$ by its integral mean.

$$\hat{\Phi}_s(s) := \frac{1}{|\partial \mathcal{D}(s)|} \int_{\partial \mathcal{D}(s)} \Phi_s. \tag{3.8}$$

Moreover, since Ω_g is thin (Assumption 1), if necessary we will extend Φ_s inside Ω_g as a constant.

3.2. REDUCTION OF THE EQUATION IN THE GAS. If we substitute equation (3.5) in equation (2.5a), we obtain:

$$\begin{aligned} \nabla \cdot (\epsilon_g \nabla \Phi_g) &= \frac{\epsilon_g}{r} \frac{\partial}{\partial r} \left(r \frac{\partial \Phi_g}{\partial r} \right) + \frac{\partial}{\partial s} \left(\epsilon_g \frac{\partial \Phi_g}{\partial s} \right) = \\ &= \epsilon_g \left(\frac{1}{r} \frac{\partial \Phi_g}{\partial r} + \frac{\partial^2 \Phi_g}{\partial r^2} \right) + \frac{d\epsilon_g}{ds} \frac{\partial \Phi_g}{\partial s} + \epsilon_g \frac{\partial^2 \Phi_g}{\partial s^2} = \\ &= \epsilon_g \left(\frac{1}{r} \frac{\partial \Phi_g}{\partial r} + \frac{\partial^2 \Phi_g}{\partial r^2} + \frac{\partial^2 \Phi_g}{\partial s^2} \right) + \frac{d\epsilon_g}{ds} \frac{\partial \Phi_g}{\partial s}. \end{aligned} \tag{3.9}$$

Since the only dependence of Φ_g on r is due to ϕ, its partial derivatives with respect to this coordinate are simply:

$$\frac{\partial \Phi_g}{\partial r} = \Phi_r \frac{d\phi}{dr} = 2r\Phi_r, \quad \frac{\partial^2 \Phi_g}{\partial r^2} = \Phi_r \frac{d^2\phi}{dr^2} = 2\Phi_r.$$

The dependence on s, instead is due to Φ_Λ and Φ_r and the corresponding partial derivatives are given by:

$$\frac{\partial \Phi_g}{\partial s} = \frac{\partial \Phi_\Lambda}{\partial s} + \frac{\partial \Phi_r}{\partial s}\phi, \quad \frac{\partial^2 \Phi_g}{\partial s^2} = \frac{d^2 \Phi_\Lambda}{ds^2} + \frac{d^2 \Phi_r}{ds^2}\phi. \tag{3.10}$$

We can substitute these expression into equation (3.9) and obtain:

$$\nabla \cdot (\epsilon_g \nabla \Phi_g) = \epsilon_g \left(4\Phi_r + \frac{d^2\Phi_\Lambda}{ds^2} + r^2 \frac{d^2\Phi_r}{ds^2} \right) + \frac{d\epsilon_g}{ds} \left(\frac{d\Phi_\Lambda}{ds} + r^2 \frac{d\Phi_r}{ds} \right), \quad \forall r < R, \ \forall s \in \Lambda, \tag{3.11}$$

which implies

$$\epsilon_g \left(4\Phi_r + \frac{d^2\Phi_\Lambda}{ds^2} + r^2 \frac{d^2\Phi_r}{ds^2} \right) + \frac{d\epsilon_g}{ds} \left(\frac{d\Phi_\Lambda}{ds} + r^2 \frac{d\Phi_r}{ds} \right) = -\frac{q(s)}{\epsilon_0}, \quad \forall r < R, \ \forall s \in \Lambda.$$

Note that this equation is not pointwise satisfied, since the left-hand side depends on r but the right-hand side does not, as a consequence of Assumption 2, neglecting the radial profile of the charge concentration q; in fact this equation is only satisfied in mean, over sections $\mathcal{D}(s), \ \forall s \in \Lambda$. Thus, we start by integrating equation (2.5a), combined with equation (3.11) over a section $\mathcal{D}$:

$$\begin{aligned} &\int_{\mathcal{D}(s)} \nabla \cdot (\epsilon_g(s) \nabla \Phi_g) = \\ &= \int_{\mathcal{D}(s)} \left[\epsilon_g(s) \left(4\Phi_r(s) + \frac{d^2\Phi_\Lambda}{ds^2}(s) + r^2 \frac{d^2\Phi_r}{ds^2}(s) \right) + \frac{d\epsilon_g}{ds}(s) \left(\frac{d\Phi_\Lambda}{ds}(s) + r^2 \frac{d\Phi_r}{ds}(s) \right) \right] \end{aligned}$$

Since the first integrand is constant over sections, while the second one depends on r, this equation becomes:

$$\begin{aligned} \int_{\mathcal{D}(s)} \nabla \cdot (\epsilon_g(s) \nabla \Phi_g) = & \\ &= |\mathcal{D}(s)| \left[\epsilon_g(s) \left(4\Phi_r(s) + \frac{d^2\Phi_\Lambda}{ds^2}(s) \right) + \frac{d\epsilon_g}{ds}(s) \frac{d\Phi_\Lambda}{ds}(s) \right] + \\ &\quad + \epsilon_g(s) \frac{d^2\Phi_r}{ds^2}(s) \int_{\mathcal{D}(s)} r^2 + \frac{d\epsilon_g}{ds}(s) \frac{d\Phi_r}{ds}(s) \int_{\mathcal{D}(s)} r^2 = \\ &= \pi R^2 \left[\epsilon_g(s) \left(4\Phi_r(s) + \frac{d^2\Phi_\Lambda}{ds^2}(s) \right) + \frac{d\epsilon_g}{ds}(s) \frac{d\Phi_\Lambda}{ds}(s) \right] + \\ &\quad + \pi \frac{R^4}{2} \left(\epsilon_g(s) \frac{d^2\Phi_r}{ds^2}(s) + \frac{d\epsilon_g}{ds}(s) \frac{d\Phi_r}{ds}(s) \right), \quad \forall s \in \Lambda. \end{aligned} \tag{3.12}$$

The continuity condition (3.6) allows us to replace Φ_r in the first term with the difference between Φ_Λ and Φ_s on the interface, where Φ_s is equivalent to its integral mean $\hat{\Phi}_s$, according to equation (3.8):

$$\begin{aligned} \pi R^2 \left[\epsilon_g(s) \left(4\Phi_r(s) + \frac{d^2\Phi_\Lambda}{ds^2}(s) \right) + \frac{d\epsilon_g}{ds}(s) \frac{d\Phi_\Lambda}{ds}(s) \right] = & \\ = \pi R^2 \left[\epsilon_g(s) \left(4\frac{\hat{\Phi}_s - \Phi_\Lambda(s)}{R^2} + \frac{d^2\Phi_\Lambda}{ds^2}(s) \right) + \frac{d\epsilon_g}{ds}(s) \frac{d\Phi_\Lambda}{ds}(s) \right]. & \end{aligned}$$

We integrate now also the right-hand side of equation (2.5a) over a section, recalling that the source term is given by the total charge $f = \frac{q(s)}{\epsilon_0}$ on $\mathcal{D}(s)$, $\forall s \in \Lambda$:

$$\int_{\mathcal{D}(s)} f = \frac{q(s)}{\epsilon_0}|\mathcal{D}(s)| = \frac{q(s)}{\epsilon_0}\pi R^2, \qquad \forall s \in \Lambda.$$

Moreover, subsituting $\frac{d}{ds}\left(\epsilon_g \frac{d\phi_\Lambda}{ds}\right) = \epsilon_g \frac{d^2\Phi_\Lambda}{ds^2} + \frac{d\epsilon_g}{ds}\frac{d\Phi_\Lambda}{ds}$ and $\frac{d}{ds}\left(\epsilon_g \frac{d\Phi_r}{ds}\right) = \epsilon_g \frac{d^2\Phi_r}{ds^2} + \frac{d\epsilon_g}{ds}\frac{d\Phi_r}{ds}$ in equation (3.12), we obtain the final formulation of the one-dimensional equation in the gas domain:

$$-\pi R^2 \frac{d}{ds}\left(\epsilon_g(s)\frac{d\Phi_\Lambda}{ds}(s)\right) + 4\pi\epsilon_g(s)\left(\Phi_\Lambda(s) - \hat{\Phi}_s(s)\right) = \pi R^2 \frac{q(s)}{\epsilon_0} + \frac{\pi R^4}{2}\frac{d}{ds}\left(\epsilon_g \frac{d\Phi_r}{ds}\right), \quad \forall s \in \Lambda.$$

Finally, since we are considering $R \to 0$, we can drop the higher order term $\frac{\pi R^4}{2}\frac{d}{ds}\left(\epsilon_g \frac{d\Phi_r}{ds}\right)$ on the right-hand side of the equation and get:

$$-\pi R^2 \frac{d}{ds}\left(\epsilon_g(s)\frac{d\Phi_\Lambda}{ds}(s)\right) + 4\pi\epsilon_g(s)\left(\Phi_\Lambda(s) - \hat{\Phi}_s(s)\right) = \pi R^2 \frac{q(s)}{\epsilon_0}, \qquad \forall s \in \Lambda. \tag{3.13}$$

The one-dimensional domain coincides with the centerline Λ of Ω_g and the boundary conditions on it must be imposed only on the two endpoints $s = 0$ and $s = S$. The interface conditions on Γ were incorporated through the previous calculations into the governing equation and resulted in a coupling reaction term. We are only left to reduce to one dimension the Dirichlet condition on $\mathcal{D}(0)$ and the interface conditions on $\mathcal{D}(S)$.

On $\mathcal{D}(0)$ we can rewrite the boundary condition introducing the splitting of Φ_g from equation (3.5):

$$\bar{\Phi}_g = \Phi_g\big|_{\mathcal{D}(0)} = \Phi_\Lambda(0) + \Phi_r(0)\phi(r) = \Phi_\Lambda(0) + \Phi_r(0)r^2, \quad r \in [0, R].$$

We can integrate over $\mathcal{D}(0)$ and obtain

$$\int_{\mathcal{D}(0)} \bar{\Phi}_g = \pi R^2 \Phi_\Lambda(0) - 2\pi \frac{R^4}{16\epsilon_0\epsilon_g} q(0).$$

If we denote by $\hat{\bar{\Phi}}_g$ the integral of $\bar{\Phi}_g$ over $\mathcal{D}(0)$:

$$\hat{\bar{\Phi}}_g := \int_{\mathcal{D}(0)} \bar{\Phi}_g,$$

we can write the boundary condition on $s = 0$ as follows:

$$\Phi_\Lambda(0) = \hat{\bar{\Phi}}_g - 2\pi \frac{R^4}{16\epsilon_0\epsilon_g} q(0).$$

Observe that $\Phi_\Lambda(0) \to \hat{\bar{\Phi}}_g$, as $R \to 0$. Then, the Dirichlet boundary condition on $s = 0$ can be approximated as:

$$\Phi_\Lambda(0) = \hat{\bar{\Phi}}_g. \tag{3.14}$$

Let us now construct a Neumann boundary condition at $s = S$ by integrating the jump condition given by equation (2.5c) on $\mathcal{D}(S)$:

$$\int_{\mathcal{D}(S)} \mathbf{D}_s \cdot \mathbf{s} = \int_{\mathcal{D}(S)} g + \int_{\mathcal{D}(S)} \epsilon_g \nabla \Phi_g \cdot \mathbf{s} = |\mathcal{D}(S)| g(S) + \int_{\mathcal{D}(S)} \epsilon_g \nabla \Phi_g \cdot \mathbf{s}.$$

We can substitute $\mathbf{D}_s$ with $-\epsilon_s \nabla \Phi_s$, and $\nabla \Phi_g \cdot \mathbf{s}$ with its expression (3.10), and the previous equation becomes:

$$\begin{aligned} -\int_{\mathcal{D}(S)} \epsilon_s \frac{\partial \Phi_s}{\partial s} &= |\mathcal{D}(S)| g(S) + |\mathcal{D}(S)| \epsilon_g(S) \frac{d\Phi_\Lambda}{ds}(S) + \epsilon_g(S) \frac{d\Phi_r}{ds}(S) \int_{\mathcal{D}(S)} \phi(r) = \\ &= \pi R^2 g(S) + \pi R^2 \epsilon_g(S) \frac{d\Phi_\Lambda}{ds}(S) + \frac{\pi R^4}{4} \epsilon_g(S) \frac{d\Phi_r}{ds}(S) \end{aligned}$$

Thanks to Assumption 1 of thin gas domain, we can approximate the potential Φ_s as a constant on the whole section, as in equation (3.8) and neglect the higher order term $\frac{\pi R^4}{4} \epsilon_g(S) \frac{d\Phi_r}{ds}(S)$:

$$-\epsilon_s \frac{d\hat{\Phi}_s}{ds}(S) = g(S) + \epsilon_g \frac{d\Phi_\Lambda}{ds}(S). \tag{3.15}$$

Collecting (3.13), (3.14) and (3.15), we obtain the 1D version of problem (2.5a)- (2.5d):

$$\begin{cases} -\pi R^2 \dfrac{d}{ds}\left(\epsilon_g \dfrac{d\Phi_\Lambda}{ds}\right) + 4\pi \epsilon_g \left(\Phi_\Lambda - \hat{\Phi}_s\right) = \pi R^2 \dfrac{q}{\epsilon_0}, & \text{on } \Lambda, \\ \Phi_\Lambda(0) = \hat{\bar{\Phi}}_g, \\ \epsilon_g \dfrac{d\Phi_\Lambda}{ds}(S) = -\epsilon_s \dfrac{d\hat{\Phi}_s}{ds}(S) - g(S). \end{cases} \tag{3.16}$$

3.3. REDUCTION OF THE PROBLEM IN THE DIELECTRIC. Consider now the problem (2.4a)-(2.4f) in the dielectric domain Ω_s in dual form, with the Robin interface condition (3.7). Since in the previous section we have reduced the gas domain to a one-dimensional line, in the final formulation of the problem obtained in this section we will extend the dielectric domain Ω_s to the whole domain Ω. Let us now define the functional spaces to which $\mathbf{D}_s$ and Φ_s belong as $H(\text{div}; \Omega)$ and $W_s := L^2(\Omega_s)$, respectively. Notice that, however, $\nabla \Phi_s = -\epsilon_s^{-1} \mathbf{D}_s \in L^2(\Omega_s)$ and therefore $\Phi_s \in H^1(\Omega_s)$. We substitute equation (2.4a) into equation (2.4b) and multiply it by a test function belonging to the same space of Φ_s, $w_s \in H^1(\Omega_s)$, and integrate by parts over Ω_s:

$$\begin{aligned} 0 = \int_{\Omega_s} \nabla \cdot \mathbf{D}_s w_s = -\int_{\Omega_s} \mathbf{D}_s \cdot \nabla w_s + \int_{\partial\Omega_{s,D}} w_s \mathbf{D}_s \cdot \mathbf{n} + \int_{\partial\Omega_{s,N}} w_s \mathbf{D}_s \cdot \mathbf{n} + \\ + \int_\Gamma w_s \mathbf{D}_s \cdot \mathbf{n}_s + \int_{\mathcal{D}(S)} w_s \mathbf{D}_s \cdot \mathbf{s}, \qquad \forall w_s \in H^1(\Omega_s). \end{aligned}$$

Imposing the Neumann boundary condition on $\partial\Omega_{s,N}$ and Assumption 4, we obtain the following expression:

$$-\int_{\Omega_s} \mathbf{D}_s \cdot \nabla w_s + \int_{\Gamma} w_s \mathbf{D}_s \cdot \mathbf{n}_s = -\int_{\partial\Omega_{s,N}} w_s \nu, \qquad \forall w_s \in H^1_{0,\partial\Omega_{s,D}}(\Omega_s), \tag{3.17}$$

where $H^1_{0,\partial\Omega_{s,D}}(\Omega_s) := \{w \in H^1(\Omega_s) \ : \ w = 0 \text{ on } \partial\Omega_{s,D}\}$. Now we can apply the Robin condition (3.7) and obtain:

$$\begin{aligned}\int_{\Gamma} w_s \mathbf{D}_s \cdot \mathbf{n}_s = \int_{\Gamma} w_s \left(g + \epsilon_g \frac{\Phi_s - \Phi_\Lambda}{\phi(R)} \phi'(R) \right) = \\ = \int_{\Lambda} g \int_{\partial\mathcal{D}} w_s + \int_{\Lambda} \epsilon_g \frac{\phi'(R)}{\phi(R)} \int_{\partial\mathcal{D}} w_s \Phi_s - \int_{\Lambda} \epsilon_g \frac{\phi'(R)}{\phi(R)} \Phi_\Lambda \int_{\partial\mathcal{D}} w_s.\end{aligned} \tag{3.18}$$

Assume that the electric potential Φ_s and the test functions $w_s \in H^1_{0,\partial\Omega_{s,D}}(\Omega_s)$ on $\partial\mathcal{D}(s),\ s \in \Lambda$, can be written as the sum of their integral mean over $\partial\mathcal{D}(s)$, which is constant on $\partial\mathcal{D}(s)$ and approximately equal to the respective mean over $\mathcal{D}(s)$, and a non-constant fluctuation around it:

$$\Phi_s = \hat{\Phi}_s + \tilde{\Phi}_s; \qquad w_s = \hat{w}_s + \tilde{w}_s, \qquad \text{on } \Gamma,$$

and make the following assumption, similar to the one made by Cerroni *et al.* [14], on the fluctuations:

Assumption 3. *The fluctuations of functions in W_s around their integral mean on $\partial\mathcal{D}(s)$ have zero mean for all $s \in \Lambda$, and so does the product of the fluctuations of two different functions in W_s, i.e.*

$$\forall v = \hat{v} + \tilde{v}, w = \hat{w} + \tilde{w} \in W_s, \qquad \int_{\partial\mathcal{D}} \tilde{w} \approx 0 \quad \textit{and} \quad \int_{\partial\mathcal{D}} \tilde{v}\tilde{w} \approx 0.$$

As a consequence, we can rewrite the integrals over $\partial\mathcal{D}$ in equation (3.18) as:

$$\int_{\partial\mathcal{D}} w_s = \int_{\partial\mathcal{D}} \hat{w}_s + \int_{\partial\mathcal{D}} \tilde{w}_s \approx \int_{\partial\mathcal{D}} \hat{w}_s = |\partial\mathcal{D}| \hat{w}_s,$$

and

$$\int_{\partial\mathcal{D}} \Phi_s w_s = \int_{\partial\mathcal{D}} \hat{w}_s \hat{\Phi}_s + \int_{\partial\mathcal{D}} \tilde{w}_s \tilde{\Phi}_s + \hat{w}_s \int_{\partial\mathcal{D}} \tilde{\Phi}_s + \hat{\Phi}_s \int_{\partial\mathcal{D}} \tilde{w}_s \approx \int_{\partial\mathcal{D}} \hat{w}_s \hat{\Phi} = |\partial\mathcal{D}| \hat{w}_s \hat{\Phi}_s.$$

We can substitute these integrals in (3.18) and back into equation (3.17) and obtain the following weak equation:

$$-\int_{\Omega_s} \epsilon_s \mathbf{D}_s \cdot \nabla w_s + \int_{\Lambda} \epsilon_g \frac{\phi'(R)}{\phi(R)} \hat{w}_s |\partial\mathcal{D}| \left(\hat{\Phi}_s - \Phi_\Lambda \right) = -\int_{\Lambda} g \hat{w}_s |\partial\mathcal{D}|, \qquad \forall w_s \in H^1_{0,\partial\Omega_{s,D}}(\Omega_s).$$

Substituting now ϕ and its derivative with their analytical expressions and $|\partial\mathcal{D}| = 2\pi R$, we obtain the final weak formulation of the primal problem in the dielectric domain:

$$\int_\Omega \epsilon_s \mathbf{D}_s \cdot \nabla w_s + 4\pi\epsilon_g \int_\Lambda \hat{w}_s \left(\Phi_\Lambda - \hat{\Phi}_s\right) = 2\pi R \int_\Lambda g\hat{w}_s, \qquad \forall w_s \in H^1_{0,\partial\Omega_{s,D}}(\Omega_s). \tag{3.19}$$

In order to go back to the strong problem and to the dual mixed formulation, we can integrate back by parts (3.19) and obtain:

$$\int_\Omega \left(-\nabla \cdot \mathbf{D}_s w_s + 4\pi\epsilon_g(\Phi_\Lambda - \hat{\Phi}_s)\hat{w}_s\delta_\Lambda\right) = \int_\Omega 2\pi R g \hat{w}_s \delta_\Lambda, \qquad \forall w_s = \hat{w}_s + \tilde{w}_s \in H^1_{0,\partial\Omega_{s,D}}(\Omega_s).$$

In particular, this holds for $w_s = \hat{w}_s$.
We have obtained a strong equation in the whole domain, with a line source term on Λ:

$$\nabla \cdot \mathbf{D}_s - 4\pi\epsilon_g(\Phi_\Lambda - \hat{\Phi}_s)\delta_\Lambda = -2\pi R g \delta_\Lambda, \qquad \text{in } \Omega.$$

If we simplify the coefficients of this equation and substitute $\mathbf{D}_s \cdot \mathbf{n}_s = -\epsilon_s \nabla\Phi_s$, we retrieve the strong dual mixed formulation of the problem in the dielectric domain with a line source concentrated on Λ and a coupling term with the 1D problem (3.16):

$$\begin{cases} \epsilon_s^{-1}\mathbf{D}_s + \nabla\Phi_s = 0, & \text{in } \Omega, \\ \nabla \cdot \mathbf{D}_s - 4\pi\epsilon_g(\Phi_\Lambda - \hat{\Phi}_s)\delta_\Lambda = -2\pi R g \delta_\Lambda, & \text{in } \Omega, \\ \Phi_s = \bar{\Phi}_s, & \text{on } \partial\Omega_D, \\ \mathbf{D}_s \cdot \mathbf{n} = \nu, & \text{on } \partial\Omega_N. \end{cases} \tag{3.20}$$

4. Reduced 3D-1D coupled problem. The final mixed-dimensional dual-primal coupled problem is the following:

$$\begin{cases} \epsilon_s^{-1}\mathbf{D}_s + \nabla\Phi_s = 0, & \text{in } \Omega, & \text{(4.1a)} \\ \nabla \cdot \mathbf{D}_s - 4\pi\epsilon_g(\Phi_\Lambda - \hat{\Phi}_s)\delta_\Lambda = -2\pi R g \delta_\Lambda, & \text{in } \Omega, & \text{(4.1b)} \\ -\pi R^2 \dfrac{d}{ds}\left(\epsilon_g \dfrac{d\Phi_\Lambda}{ds}\right) + 4\pi\epsilon_g\left(\Phi_\Lambda - \hat{\Phi}_s\right) = \pi R^2 \dfrac{q}{\epsilon_0} & \text{on } \Lambda, & \text{(4.1c)} \\ \Phi_\Lambda(0) = \hat{\bar{\Phi}}_g, & & \text{(4.1d)} \\ \epsilon_g \dfrac{d\Phi_\Lambda}{ds}(S) = -g(S) - \epsilon_s \dfrac{d\hat{\Phi}_s}{ds}(S), & & \text{(4.1e)} \\ \Phi_s = \bar{\Phi}_s, & \text{on } \partial\Omega_D, & \text{(4.1f)} \\ \mathbf{D}_s \cdot \mathbf{n} = \nu, & \text{on } \partial\Omega_N. & \text{(4.1g)} \end{cases}$$

Note that, despite the differences in the derivation, similar coupling terms between problems in mixed-dimensional domains can also be found in the context of fluid flow, [30] [23].

We can observe that not only is a coupling between the problems in the two domains present in the equations (4.1b) and (4.1c), but also it appears at the tip of the one-dimensional reduced domain

as a Neumann condition, similar to the jump interface condition (2.3a). However, the value of the coefficient $4\pi\epsilon_g$ makes the coupling term in equation (4.1c) predominant in the evolution of Φ_g and the coupling at the tip of Λ negligible. Moreover, since the area $\mathcal{D}(S)$ is small, according to Assumption 1, we can assume that the flux exchange between the gas and the dielectric domain happens mostly through the lateral surface Γ of Ω_g and the contribution across $\mathcal{D}(S)$ is negligible:

Assumption 4. *The flux of the electric field across $\mathcal{D}(S)$ is negligible, i.e. $\int_{\mathcal{D}(S)} \nabla\Phi_s \cdot \mathbf{s} \approx 0$.*

This way we obtain an alternative boundary condition for the 1D problem, which is simply:

$$\frac{d\Phi_\Lambda}{ds}(S) = -\frac{1}{\epsilon_g} g(S). \tag{4.2}$$

Remark 1. *Alternatively, we could also choose to substitute the coupling term in equations* (4.1b) *and* (4.1c) *by the known quantity $\Phi_r\phi(R)$, as in* (3.6)*. In this case, we would not be allowed to rely on Assumption 4 without actually decoupling the two problems, and we would need keep condition* (4.1e) *as it is, introducing a weak coupling at the tip of the 1D domain. Moreover, in this case we would not be imposing the condition* (3.6) *of continuity of the potentials across the interface Γ between the two original domains, and should take it into account as one additional equation.*

Remark 2. *Under the Assumptions 1, 2, 3, the effect of a uniform volume charge distribution in a cylinder and of a line charge distribution on its centerline are equivalent outside of Ω_g. Indeed, the flux of the displacement field $\mathbf{D}_s$ on a cylindrical surface $\partial\mathcal{W}$ surrounding Ω_g remains the same in the two cases. We can compute it by applying the Gauss theorem to the original 3D-3D problem, taking into account Assumption 2 of constant charge over sections of Ω_g:*

$$\int_{\partial\mathcal{W}} \mathbf{D}_s \cdot \mathbf{n} = \int_{\mathcal{W}} \frac{q}{\epsilon_0} = \int_\Lambda \frac{q}{\epsilon_0} |\mathcal{B}|, \tag{4.3}$$

where $\mathcal{B}$ denotes a transversal section of $\mathcal{W}$. If we do the same on the reduced 3D-1D problem, we obtain:

$$\int_{\partial\mathcal{W}} \mathbf{D}_s \cdot \mathbf{n} = \int_{\mathcal{W}} \frac{q}{\epsilon_0}\delta_\Lambda = \int_\Lambda \frac{q}{\epsilon_0} |\mathcal{B}|,$$

which is equivalent to equation (4.3)*.*

4.1. WELL-POSEDNESS OF THE DUAL-PRIMAL PROBLEM. In this section we will prove that the coupled 3D-1D problem (4.1a)- (4.1g) admits a unique weak solution.
A similar problem, in primal form, was proven to be well-posed by D'angelo and Quarteroni [17] on weighted Sobolev spaces. As we will see in the following section, we do not need to define a continuous trace operator and, consequently, to work with such spaces.
The well-posedness of a similar problem in mixed dimensions was also studied by Březina and Exner [9], where however the one-dimensional equation is not expressed in primal form, as we have in equation (4.1c). Mixed-dimensional problems in dual-primal form can be found in [19] and [1], but defined on subdomains of codimension 1.

We start by gathering the weak formulation of problem (4.1a)-(4.1g), imposing the Neumann boundary condition on $\partial\Omega_N$ with the Lagrange multiplier $\xi = -\mathbf{D}_s \cdot \mathbf{n}\big|_{\partial\Omega_N}$. Let us define the following spaces:

$$H^{1/2}(\partial\Omega_N) = \{\phi\big|_{\partial\Omega_N} \ : \ \phi \in H^1(\Omega)\};$$

$$W_\Lambda = H^1(\Lambda) = \left\{\psi \in L^2(\Lambda) \ : \ \frac{d\psi}{ds} \in L^2(\Lambda)\right\};$$

$$W_s = L^2(\Omega);$$

$$V_s = \{\mathbf{v} \in H(\mathrm{div};\Omega) \ : \ \mathbf{v}\cdot\mathbf{n} \in L^2(\partial\Omega)\},$$

where V_s is a subspace of $H(\mathrm{div};\Omega) = \{\mathbf{v} \in L^2(\Omega) \ : \ \nabla\cdot\mathbf{v} \in L^2(\Omega)\}$ that takes into account the boundary conditions on $\partial\Omega_N$. Note that we have required extra regularity on the trace of $\mathbf{v}\cdot\mathbf{n}$ on the boundary.
On these spaces we consider the norms $\|\lambda\|_{H^{1/2}(\partial\Omega_N)} = \inf\{\|\phi\|_{H^1(\Omega)} \ : \ \phi \in H^1(\Omega), \ \phi\big|_{\partial\Omega_N} = \lambda\}$, $\|\psi\|_{W^0_\Lambda} = \|\psi\|_{L^2(\Lambda)}$, $\|\phi\|_{W_s} = \|\phi\|_{H^1(\Omega)}$ and $\|\mathbf{v}\|^2_{V_s} = \|\nabla\cdot\mathbf{v}\|^2_{L^2(\Omega)} + \|\mathbf{v}\|^2_{L^2(\Omega)} + \|\mathbf{v}\cdot\mathbf{n}\|^2_{L^2(\partial\Omega)}$.

If we integrate by parts equations (4.1a)-(4.1c), substitute the boundary conditions (4.1d)-(4.1g) and exploit Assumption 3, as in the derivation of equation (3.19), we obtain the following problem:

Find $((\mathbf{D}_s,\xi),\Phi_s,\Phi_\Lambda) \in \left(V_s \times H^{1/2}(\partial\Omega_N)\right) \times W_s \times W_\Lambda$ such that:

$$\begin{cases} A(\mathbf{D}_s,\mathbf{v}) + \mathcal{B}(\mathbf{v},(\Phi_s,\xi)) = -<\bar{\Phi}_s, \mathbf{v}\cdot\mathbf{n}>_{\partial\Omega_D}, & \forall \mathbf{v} \in V_s, \quad (4.4a)\\ \mathcal{B}(\mathbf{v},(\phi,\lambda)) + c_{\Lambda s}(\Phi_\Lambda,\hat{\phi}) - c_{ss}(\hat{\Phi}_s,\hat{\phi}) =< G,\hat{\phi}>_\Lambda - <\nu,\phi>_{\partial\Omega_N}, & \forall \phi \in W_s, \forall \lambda \in H^{1/2}(\partial\Omega_N), \quad (4.4b)\\ \mathcal{A}_\Lambda(\Phi_\Lambda,\psi) + c_{\Lambda\Lambda}(\Phi_\Lambda,\psi) - c_{\Lambda s}(\hat{\Phi}_s,\psi) =< F,\psi>_\Lambda, & \forall \psi \in W^0_\Lambda, \quad (4.4c) \end{cases}$$

where we have defined the following operators:

$$\begin{aligned}
\mathcal{A} \ : \quad & V_s \times V_s \longrightarrow \mathbb{R}, && \mathcal{A}(\mathbf{u},\mathbf{v}) = \epsilon_s^{-1}\int_\Omega \mathbf{u}\cdot\mathbf{v};\\
\mathcal{B} \ : \quad & V_s \times \left(W_s \times H^{1/2}(\partial\Omega_N)\right) \longrightarrow \mathbb{R}, && \mathcal{B}(\mathbf{u},(\phi,\lambda)) = -\int_\Omega \phi\nabla\cdot\mathbf{u} + \int_{\partial\Omega_N}\lambda\mathbf{v}\cdot\mathbf{n};\\
c_{\Lambda\Lambda} \ : \quad & W_\Lambda \times W_\Lambda \longrightarrow \mathbb{R}, && c_{\Lambda\Lambda}(\psi_1,\psi_2) = 4\pi\epsilon_g\int_\Lambda \psi_1\psi_2;\\
c_{\Lambda s} \ : \quad & W_\Lambda \times W_s \longrightarrow \mathbb{R}, && c_{\Lambda,s}(\psi,\phi) = 4\pi\epsilon_g\int_\Lambda \psi\hat{\phi};\\
c_{ss} \ : \quad & W_s \times W_s \longrightarrow \mathbb{R}, && c_{ss}(\phi_1,\phi_2) = 4\pi\epsilon_g\int_\Lambda \hat{\phi}_1\hat{\phi}_2;\\
\mathcal{A}_\Lambda \ : \quad & W_\Lambda \times W_\Lambda \longrightarrow \mathbb{R}, && \mathcal{A}_\Lambda(\phi,\psi) = \pi R^2\int_\Lambda \epsilon_g\frac{d\psi}{ds}\frac{d\phi}{ds};\\
G \ : \quad & \Lambda \longrightarrow \mathbb{R}, && G = \frac{g}{2\epsilon_g}R;\\
F \ : \quad & \Lambda \longrightarrow \mathbb{R}, && F = \pi R^2\frac{q}{4\epsilon_0}.
\end{aligned}$$

We assume that $g \in L^2(\Lambda)$, $q \in L^2(\Lambda)$, $\bar{\Phi}_s \in H^{-1/2}(\partial\Omega_D)$, $\nu \in H^{-1/2}(\partial\Omega_N)$, $\epsilon_g \in L^\infty(\Lambda)$, $\epsilon_s \in L^\infty(\Omega)$ and $\epsilon_s \geq \epsilon_g \geq 1$.
If we sum equation (4.4c) and equation (4.4a), we obtain the following equivalent problem:

Find $\left((\mathbf{D}_s, \Phi_\Lambda), (\Phi_s, \xi)\right) \in \left((V_s \times W_\Lambda) \times \left(W_s \times H^{1/2}(\partial\Omega_N)\right)\right)$ such that:

$$\begin{cases} a\left((\mathbf{D}_s, \Phi_\Lambda), (\mathbf{v}, \psi)\right) + b_1\left((\mathbf{v}, \psi), (\Phi_s, \xi)\right) = - < \bar{\Phi}_s, \mathbf{v} \cdot \mathbf{n} >_{\partial\Omega_D} + < F, \psi >_\Lambda, \\ \qquad\qquad\qquad\qquad\qquad\qquad\qquad\qquad \forall\, (\mathbf{v}, \psi) \in V_s \times W_\Lambda, \\ b_2\left((\mathbf{D_s}, \Phi_\Lambda), (\phi, \lambda)\right) - c_{ss}\left(\Phi_s, \phi\right) =< G, \hat{\phi} >_\Lambda - < \nu, \phi >_{\partial\Omega_N}, \\ \qquad\qquad\qquad\qquad\qquad\qquad\qquad\qquad \forall (\phi, \lambda) \in W_s \times H^{1/2}(\partial\Omega_N). \end{cases} \tag{4.5}$$

where we define a norm over the product spaces $V_s \times W_\Lambda$ and $W_s \times H^{1/2}(\partial\Omega_N)$ respectively as:

$$\| (\mathbf{v}, \psi) \|_{V_s \times W_\Lambda} = \sqrt{\|\mathbf{v}\|^2_{V_2} + \|\psi\|^2_{W_\Lambda}},$$
$$\| (\phi, \xi) \|_{W_s \times H^{1/2}(\partial\Omega_N)} = \sqrt{\|\phi\|^2_{W_s} + \|\xi\|^2_{H^{1/2}(\partial\Omega_N)}}$$

and the operators $a : (V_s \times W_\Lambda) \times (V_s \times W_\Lambda) \to \mathbb{R}$, $b_1 : (V_s \times W_\Lambda) \times \left(W_s \times H^{1/2}(\partial\Omega_N)\right) \to \mathbb{R}$ and $b_2 : (V_s \times W_\Lambda) \times \left(W_s \times H^{1/2}(\partial\Omega_N)\right) \to \mathbb{R}$ respectively as follows:

$$\begin{aligned} a\left((\mathbf{v}_1, \psi_1), (\mathbf{v}_2, \psi_2)\right) &= \mathcal{A}_s(\mathbf{v}_1, \mathbf{v}_2) + \mathcal{A}_\Lambda(\psi_1, \psi_2) + c_{\Lambda\Lambda}(\psi_1, \psi_2), \\ b_1\left((\mathbf{v}, \psi), (\phi, \xi)\right) &= \mathcal{B}(\mathbf{v}, (\phi, \xi)) - c_{\Lambda s}(\psi, \phi), \\ b_2\left((\mathbf{v}, \psi), (\phi, \xi)\right) &= \mathcal{B}(\mathbf{v}, (\phi, \xi)) + c_{\Lambda s}(\psi, \phi). \end{aligned}$$

We can prove that this saddle point problem admits a unique solution, relying on the results by Nicolaides [29], Bernardi *et al.* [7], Brezzi and Fortin [11].

In order to show this result, we need to prove that the integral mean of a function in $L^2(\Omega)$ belongs to $L^2(\Lambda)$, and we do it in a similar way as Cerroni *et al.* [14].

Lemma 1. *If $\phi \in L^2(\Omega)$, then $\hat{\phi} \in L^2(\Lambda)$ and $\exists k > 0$ such that the following inequality holds:*

$$\|\hat{\phi}\|^2_{L^2(\Lambda)} \leq k \|\phi\|^2_{L^2(\Omega)}.$$

Proof. By definition of the L^2-space, $\hat{\phi} \in L^2(\Lambda) \iff \int_\Lambda \hat{\phi}^2 ds < \infty$. Then, we consider

$$\int_\Lambda \hat{\phi}^2 ds = \int_\Lambda \left(\frac{1}{|\mathcal{D}(s)|} \int_{\mathcal{D}(s)} \phi \right)^2. \tag{4.6}$$

By Jensen's inequality,

$$\left(\frac{1}{|\mathcal{D}(s)|} \int_{\mathcal{D}(s)} \phi \right)^2 \leq \frac{1}{|\mathcal{D}(s)|^2} \int_{\mathcal{D}(s)} \phi^2,$$

the right-hand side of equation (4.6) can be rewritten as follows:

$$\int_\Lambda \left(\frac{1}{|\mathcal{D}(s)|} \int_{\mathcal{D}(s)} \phi \right)^2 \leq \int_\Lambda \frac{1}{|\mathcal{D}(s)|^2} \int_{\mathcal{D}(s)} \phi^2.$$

Observe that the double integral over $\Lambda \times \mathcal{D}(s)$ is equivalent to the integral of ϕ over Ω_g and, as we assume $|\mathcal{D}(s)| = \pi R^2,\ \forall s \in \Lambda$, then, we have

$$\int_\Lambda \hat{\phi}^2 ds \leq \frac{1}{|\mathcal{D}(s)|^2} \int_{\Omega_g} \phi^2 = \frac{1}{(\pi R^2)^2} \int_{\Omega_g} \phi^2 \leq \frac{1}{(\pi R^2)^2} \int_\Omega \phi^2 = \frac{1}{(\pi R^2)^2} \|\phi\|^2_{L^2(\Omega)} < \infty,$$

since $\phi^2 \geq 0$ and $\Omega_g \subset \Omega$.

We have proved that $\hat{\phi} \in L^2(\Lambda)$ and $\|\hat{\phi}\|^2_{L^2(\Lambda)} \leq k\|\phi\|^2_{L^2(\Omega)}$, with $k = \dfrac{1}{(\pi R^2)^2}$. □

We also need to prove some results on the operators involved in the problem that will allow us to show the well-posedness of (4.1a)-(4.1g).

Lemma 2. *G and F belong to $L^2(\Lambda)$ and the right-hand sides of the equations* (4.5) *are continuous.*

Proof. A straightforward consequence of the assumption $g, q \in L^2(\Lambda)$ is that also G and F belong to $L^2(\Lambda)$.
For the continuity, we start by applying the triangular inequality and Cauchy-Schwarz inequality:

$$\begin{aligned} | < G, \hat{\phi} >_\Lambda - < \nu, \phi >_{\partial\Omega_N} | \leq | < G, \hat{\phi} >_\Lambda | + | < \nu, \phi >_{\partial\Omega_N} | \leq \\ \leq \|G\|_{L^2(\Lambda)} \|\hat{\phi}\|_{L^2(\Lambda)} + \|\nu\|_{H^{-1/2}(\partial\Omega_N)} \|\phi\|_{H^{1/2}(\partial\Omega_N)}, \qquad \forall \phi \in W_s. \end{aligned}$$

By Lemma 1,

$$\begin{aligned} | < G, \hat{\phi} >_\Lambda + < \nu, \phi >_{\partial\Omega_N} | \leq \max\left\{ \frac{\|G\|_{L^2(\Lambda)}}{\pi R^2}, \|\nu\|_{H^{-1/2}(\partial\Omega_N)} \right\} \|\phi\|_{H^1(\Omega)} \leq \\ \leq \max\left\{ \frac{\|G\|_{L^2(\Lambda)}}{\pi R^2}, \|\nu\|_{H^{-1/2}(\partial\Omega_N)} \right\} \| (\phi, \psi) \|_{W_s \times W_\Lambda}, \qquad \forall (\phi, \xi) \in W_s \times H^{1/2}(\partial\Omega_N). \end{aligned}$$

Finally, by triangular inequality and Cauchy-Schwarz inequality,

$$\begin{aligned} \left| - < \bar{\Phi}_s, \mathbf{v} \cdot \mathbf{n} >_{\partial\Omega_D} + < F, \psi >_\Lambda \right| \leq \|\bar{\Phi}_s\|_{L^2(\partial\Omega_D)} \|\mathbf{v} \cdot \mathbf{n}\|_{L^2(\partial\Omega_D)} + \|F\|_{L^2(\Lambda)} \|\psi\|_{L^2(\Lambda)} \leq \\ \leq \|\bar{\Phi}_s\|_{L^2(\partial\Omega_D)} \|\mathbf{v}\|_{V_s} + \|F\|_{L^2(\Lambda)} \|\psi\|_{L^2(\Lambda)} \leq \max\left\{ \|\bar{\Phi}_s\|_{L^2(\partial\Omega_D)}, \|F\|_{L^2(\Lambda)} \right\} \|\mathbf{v}, \psi\|_{V_s \times W_\Lambda}, \\ \forall\, (\mathbf{v}, \psi) \in V_s \times W_\Lambda. \end{aligned}$$

□

Lemma 3. *The bilinear form a is positive definite, i.e.*

$$a\left((\mathbf{u}_1, \psi_1), (\mathbf{u}_2, \psi_2)\right) > 0,\ \forall\, (\mathbf{u}_1, \psi_1),\ (\mathbf{u}_2, \psi_2) \in V_s,$$

continuous and coercive on the kernel of b_1 and of b_2,

$$\ker(b_1) = \ker(b_2) = \ker(b) = \{(\mathbf{u}, \psi) \in V_s \times W_s\ :\ \nabla \cdot \mathbf{u} = 0,\ \mathbf{u} \cdot \mathbf{n} = 0 \text{ on } \partial\Omega_N\}. \tag{4.7}$$

Proof. For the continuity, by triangular and Cauchy-Schwarz inequality,

$$|a\left((\mathbf{u}_1,\psi_1),(\mathbf{u}_2,\psi_2)\right)| = \left|\epsilon_s^{-1}\int_\Omega \mathbf{u}_1\cdot\mathbf{u}_2 + \int_\Lambda \pi R^2\epsilon_g\frac{d\psi_1}{ds}\frac{d\psi_2}{ds} + 4\pi\epsilon_g\psi_1\psi_2\right| \leq$$
$$\leq (\min_\Omega(\epsilon_s))^{-1}\|\mathbf{u}_1\|_{L^2(\Omega)}\|\mathbf{u}_2\|_{L^2(\Omega)} + \pi R^2\max_\Lambda(\epsilon_g)|\psi_1|_{H^1(\Omega)}|\psi_2|_{H^1(\Omega)} +$$
$$+ 4\pi\max_\Lambda(\epsilon_g)\|\psi_1\|_{L^2(\Lambda)}\|\psi_2\|_{L^2(\Lambda)}$$

Moreover, exploiting the definitions of the norms in V_s and W_Λ and on their product space:

$$|a\left((\mathbf{u}_1,\psi_1),(\mathbf{u}_2,\psi_2)\right)| \leq K_1\left(\|\mathbf{u}_1\|_{L^2(\Omega)}\|\mathbf{u}_2\|_{L^2(\Omega)} + \|\psi_1\|_{H^1(\Lambda)}\|\psi_2\|_{H^1(\Lambda)}\right) \leq$$
$$\leq K_1\|\left(\mathbf{u}_1,\psi_1\right)\|_{V_s\times W_\Lambda}\|\left(\mathbf{u}_2,\psi_2\right)\|_{V_s\times W_\Lambda}, \qquad \forall\left(\mathbf{u},\psi\right)\in V_s\times W_\Lambda,$$

with $K_1 > 0$.
Moreover, by definition of the norms in V_s and W_Λ and on their product space and recalling that $\mathbf{u}\in\ker(b)$ implies $\nabla\cdot\mathbf{u}=0$, $\mathbf{u}\cdot\mathbf{n}=0$, and thus $\|\mathbf{u}\|_{V_s} = \|\mathbf{u}\|_{L^2(\Omega)}$, $\forall\mathbf{u}\in\ker(b)$, we conclude that a is coercive on $\ker(b)$:

$$\begin{aligned} a\left((\mathbf{u},\psi),(\mathbf{u},\psi)\right) &\geq \|\epsilon_s\|^{-1}_{L^\infty(\Omega)}\int_\Omega|\mathbf{u}|^2 + \int_\Lambda \pi R^2\min_\Lambda(\epsilon_g)\left(\frac{d\psi}{ds}\right)^2 + \int_\Lambda 4\pi\min_\Lambda(\epsilon_g)\psi^2 \geq \\ &\geq \|\epsilon_s\|^{-1}_{L^\infty(\Omega)}\|\mathbf{u}\|^2_{L^2(\Omega)} + \pi R^2\|\nabla\psi\|^2_{H^1(\Lambda)} + 4\pi\|\psi\|^2_{L^2(\Lambda)} \geq \\ &\geq K_2\left(\|\left(\mathbf{u},\psi\right)\|_{V_s\times W_\Lambda}\right), \qquad \forall\left(\mathbf{u},\psi\right)\in\ker(b), \end{aligned} \tag{4.8}$$

with $K_2 > 0$.
Finally, a is also positive definite, as a consequence of equation (4.8):

$$a\left((\mathbf{u},\psi),(\mathbf{u},\psi)\right) \geq \|\epsilon_s\|^{-1}_{L^\infty(\Omega)}\|\mathbf{u}\|^2_{L^2(\Omega)} + \pi R^2\min_\Lambda(\epsilon_g)\|\nabla\psi\|^2_{H^1(\Lambda)} + 4\pi\min_\Lambda(\epsilon_g)\|\psi\|^2_{L^2(\Lambda)} \geq 0,$$
$$\forall\left(\mathbf{u},\psi\right)\in V_s\times W_\Lambda.$$

□

Lemma 4. *The operators b_1 and b_2 are continuous.*

Proof. By triangular and Cauchy-Schwarz inequality,

$$|b_1\left((\mathbf{u},\psi),(\phi,\xi)\right)| = \left|-\int_\Omega\phi\nabla\cdot\mathbf{u} + \int_{\partial\Omega_N}\xi\mathbf{u}\cdot\mathbf{n} - \int_\Lambda\psi\hat{\phi}\right| \leq$$
$$\leq \|\phi\|_{L^2(\Omega)}\|\nabla\cdot\mathbf{u}\|_{L^2(\Omega)} + \|\xi\|_{H^{1/2}(\partial\Omega_N)}\|\mathbf{u}\cdot\mathbf{n}\|_{L^2(\Omega)} + \|\psi\|_{L^2(\Omega)}\|\hat{\phi}\|_{L^2(\lambda)}. \tag{4.9}$$

and the same holds for b_2:

$$|b_2\left((\mathbf{u},\psi),(\phi,\xi)\right)| = \left|-\int_\Omega\phi\nabla\cdot\mathbf{u} + \int_{\partial\Omega_N}\xi\mathbf{u}\cdot\mathbf{n} + \int_\Lambda\psi\hat{\phi}\right| \leq$$
$$\leq \|\phi\|_{L^2(\Omega)}\|\nabla\cdot\mathbf{u}\|_{L^2(\Omega)} + \|\xi\|_{H^{1/2}(\partial\Omega_N)}\|\mathbf{u}\cdot\mathbf{n}\|_{L^2(\Omega)} + \|\psi\|_{L^2(\Omega)}\|\hat{\phi}\|_{L^2(\lambda)}. \tag{4.10}$$

By exploiting the definition of the norms in V_s, W_s and W_Λ and Lemma 1, we can show that b is continuous:

$$|b_i\left((\mathbf{u},\psi),(\phi,\xi)\right)| \leq \|\phi\|_{W_s}\|\mathbf{u}\|_{V_s} + \|\xi\|_{H^{1/2}(\partial\Omega_N)}\|\mathbf{u}\cdot\mathbf{n}\|_{V_s} + \|\psi\|_{W_\Lambda}\frac{\|\phi\|_{L^2(\Omega)}}{\pi R^2} \leq$$
$$\leq K_3\|\left(\mathbf{u},\psi\right)\|_{V_s\times W_\Lambda}\|\left(\phi,\xi\right)\|_{W_s\times H^{1/2}(\partial\Omega_N)}, \quad i=1,2,$$

with $K_3>0$. □

Lemma 5. *The bilinear forms* $b_i,\ i=1,2$, *satisfy the* $\inf-\sup$ *condition:*

$$\exists K_i>0 \text{ such that } \sup_{\substack{(\mathbf{v},\psi)\in V_s\times W_\Lambda\\ \mathbf{v}\neq\mathbf{0},\ \psi\neq 0}} \frac{b_i\left((\mathbf{v},\psi),(\phi,\lambda)\right)}{\|\left(\mathbf{v},\psi\right)\|_{V_s\times W_\Lambda}} \geq K_i\|(\phi,\lambda)\|_{W_s\times H^{1/2}(\partial\Omega_N)},$$
$$\forall(\phi,\lambda)\in W_s\times H^{1/2}(\partial\Omega_N),\ i=1,2. \quad (4.11)$$

Proof. As in [3], we first prove that $\exists C_1>0$ such that

$$\sup_{\substack{(\mathbf{v},\psi)\in V_s\times W_\Lambda\\ \mathbf{v}\neq\mathbf{0},\ \psi\neq 0}} \frac{b_i\left((\mathbf{v},\psi),(\phi,\lambda)\right)}{\|\left(\mathbf{v},\psi\right)\|_{V_s\times W_\Lambda}} \geq C_1\|\phi\|_{W_s}, \quad \forall\phi,\in W_s \quad (4.12)$$

and then that $\exists C_2>0$ such that

$$\sup_{\substack{(\mathbf{v},\psi)\in V_s\times W_\Lambda\\ \mathbf{v}\neq\mathbf{0},\ \psi\neq 0}} \frac{b_i\left((\mathbf{v},\psi),(\phi,\lambda)\right)}{\|\left(\mathbf{v},\psi\right)\|_{V_s\times W_\Lambda}} \geq K\|\mu\|_{H^{1/2}(\partial\Omega_N}, \quad \forall\mu\in H^{1/2}(\partial\Omega_N). \quad (4.13)$$

Finally, according to Theorem 3.1 of [20], (4.12) and (4.13) are necessary and sufficient conditions for (4.11).
Let $(\phi,\lambda)\in W_s\times H^{1/2}(\partial\Omega_N)$ and $z\in H^1(\Omega)$ be the solution to

$$\begin{cases} -\Delta z=\phi, & \text{in } \Omega\\ z=0, & \text{on } \partial\Omega_D,\\ \nabla z\cdot\mathbf{n}=0, & \text{on } \partial\Omega_N,\ i=1,2. \end{cases}$$

Fixed $\tilde{\mathbf{v}}\in V_s$ such that $\tilde{\mathbf{v}}=\nabla z$, then $-\nabla\cdot\tilde{\mathbf{v}}=\phi$, $\tilde{\mathbf{v}}\cdot\mathbf{n}=0$ on $\partial\Omega_N$.
Moreover, $\|\tilde{\mathbf{v}}\|_{L^2(\Omega)}\leq\|z\|_{L^2(\Omega)}\leq C\|\phi\|_{L^2(\Omega)}$ for some $C>0$, by continuity of the solution to the Laplace problem.
Let $w\in H^1(\Lambda)$ be the solution to

$$\begin{cases} -\dfrac{d^2w}{ds^2} &= \hat{\phi}, \quad \text{on } \Lambda,\\ w(0) &= 0,\\ \dfrac{dw}{ds}(S) &= 0. \end{cases} \quad (4.14)$$

Fixed $\tilde{\psi}_i\in W_s,\ i=1,2$, such that $\tilde{\psi}_2=w$ and $\tilde{\psi}_1=-w$, the continuous dependence of the solution to problem (4.14) implies $\|\tilde{\psi}_i\|_{H^1(\Lambda)}\leq C_i\|\hat{\phi}\|_{L^2(\Lambda)}$, for some $C_i>0$, $i=1,2$. As a

consequence, by Lemma 1, $\|\psi_1\|_{H^1(\Lambda)} = \|\psi_1\|_{W_\Lambda} \leq \dfrac{\|\phi\|_{L^2(\Omega)}}{\pi R^2},\ i = 1, 2.$
Then,

$$\sup_{\substack{(\mathbf{v},\psi)\in V_s\times W_\Lambda\\ \mathbf{v}\neq\mathbf{0}\\ \psi\neq 0}} \frac{b_i\left((\mathbf{v},\psi),(\phi,\lambda)\right)}{\|(\mathbf{v},\psi)\|_{V_s\times W_\Lambda}} = \frac{b_i\left(\left(\tilde{\mathbf{v}},\tilde{\psi}_i\right),(\phi,\lambda)\right)}{\|\left(\tilde{\mathbf{v}},\tilde{\psi}_i\right)\|_{V_s\times W_\Lambda}} =$$

$$= \frac{1}{\left(\|\tilde{\mathbf{v}}\|^2_{V_s} + \|\tilde{\psi}_i\|^2_{W_\Lambda}\right)^{1/2}}\left(-\int_\Omega \phi\nabla\cdot\tilde{\mathbf{v}} + \int_{\partial\Omega_N}\lambda\tilde{\mathbf{v}}\cdot\mathbf{n} - \int_\Lambda \tilde{\psi}_i\frac{d^2\tilde{\psi}_i}{ds^2}\right) \geq$$

$$\geq \frac{1}{C\|\phi\|_{W_s}}\left(-\int_\Omega \phi^2 - \int_\Lambda \tilde{\psi}_i\frac{d^2\tilde{\psi}_i}{ds^2}\right), \quad \forall(\phi,\lambda)\in W_s\times H^{1/2}(\partial\Omega_N),\ i=1,2. \tag{4.15}$$

We can integrate the last term by parts and apply boundary conditions of problem (4.14):

$$-\int_\Lambda \tilde{\psi}\frac{d^2\tilde{\psi}}{ds^2} = \int_\Lambda\left(\frac{d\tilde{\psi}}{ds}\right)^2 - \left(\tilde{\psi}(S)\frac{d\tilde{\psi}}{ds}(S) - \tilde{\psi}(0)\frac{d\tilde{\psi}}{ds}(0)\right) = \left\|\frac{d\tilde{\psi}}{ds}\right\|^2_{L^2(\Lambda)}.$$

If we substitute the equation above in equation (4.16), we obtain (4.12):

$$\sup_{\substack{(\mathbf{v},\psi)\in V_s\times W_\Lambda\\ \mathbf{v}\neq\mathbf{0}\\ \psi\neq 0}} \frac{b_i\left((\mathbf{v},\psi),(\phi,\lambda)\right)}{\|(\mathbf{v},\psi)\|_{V_s\times W_\Lambda}} \geq \frac{1}{C\|\phi\|_{W_s}}\left(\|\phi\|^2_{W_s} + \left\|\frac{d\tilde{\psi}_i}{ds}\right\|^2_{L^2(\Lambda)}\right) \geq C_1\|\phi\|_{W_s},$$

$$\forall(\phi,\lambda)\in W_s\times H^{1/2}(\partial\Omega_N),\ i=1,2.$$

Let now $\nu\in H^{-1/2}(\partial\Omega_N)$ and $t\in H^1(\Omega)$ be the solution to

$$\begin{cases} -\Delta t = 0, & \text{in } \Omega\\ t = 0, & \text{on } \partial\Omega_D,\\ \nabla t\cdot\mathbf{n} = \nu, & \text{on } \partial\Omega_N. \end{cases}$$

Fixed $\hat{\mathbf{v}}\in V_s$ such that $\hat{\mathbf{v}} = -\nabla t$, then $\nabla\cdot\hat{\mathbf{v}} = 0$, $-\hat{\mathbf{v}}\cdot\mathbf{n} = \nu$ on $\partial\Omega_N$.
Moreover, $\|\hat{\mathbf{v}}\|_{L^2(\Omega)} \leq \|t\|_{H^1(\Omega)} \leq C_2\|\nu\|_{H^{-1/2}(\partial\Omega_N)}$ for some $C>0$, by continuity of the solution to the Poisson problem, and consequently $\|\hat{\mathbf{v}}\|^2_{V_s} = \|\hat{\mathbf{v}}\|^2_{L^2(\Omega)} + \|\nu\|^2_{H^{-1/2}(\partial\Omega_N} \leq (1+C^2)\|\nu\|^2_{H^{-1/2}(\partial\Omega_N}$.
Then, we can repeat the same steps as before and apply the Poincaré inequality to $\|\psi\|_{H^1(\Omega)}$ and Riesz representation theorem to $<\lambda,\nu>_{\partial\Omega_N}$:

$$\sup_{\substack{(\mathbf{v},\psi)\in V_s\times W_\Lambda\\ \mathbf{v}\neq\mathbf{0}\\ \psi\neq 0}} \frac{b_i\left((\mathbf{v},\psi),(\phi,\lambda)\right)}{\|(\mathbf{v},\psi)\|_{V_s\times W_\Lambda}} = \frac{b_i\left(\left(\tilde{\mathbf{v}},\tilde{\psi}_i\right),(\phi,\lambda)\right)}{\|\left(\tilde{\mathbf{v}},\tilde{\psi}_i\right)\|_{V_s\times W_\Lambda}} = \frac{<\lambda,\nu>_{\partial\Omega_N} + \left\|\frac{d\tilde{\psi}_i}{ds}\right\|^2_{L^2(\Lambda)}}{\left(C\|\nu\|^2_{H^{-1/2}(\partial\Omega_N)} + \|\tilde{\psi}_i\|^2_{W_\Lambda}\right)^{1/2}} \geq$$

$$\geq \frac{1}{\left(C\|\lambda\|^2_{H^{1/2}(\partial\Omega_N)} + \left(1+C_p^2\right)\left\|\frac{d\tilde{\psi}_i}{ds}\right\|^2_{L^2(\lambda)}\right)^{1/2}} \left(\|\lambda\|^2_{H^{1/2}(\partial\Omega_N)} + \left\|\frac{d\tilde{\psi}_i}{ds}\right\|^2_{L^2(\Lambda)}\right) \geq C_2\|\lambda\|_{H^{1/2}(\partial\Omega_N)},$$

$$\forall(\phi,\lambda)\in W_s\times H^{1/2}(\partial\Omega_N),\ i=1,2. \tag{4.16}$$

This proves (4.13), which, together with (4.12), implies (4.11). □

Lemma 6. *The operator c_{ss} is positive semi-definite and symmetric.*

Proof. Symmetry is straightforward, since it is defined as the integral of a product.

Consider now $\phi\in W_s$:

$$c_{ss}(\phi,\phi) = 4\pi\epsilon_g\int_\Lambda \hat{\phi}^2 = 4\pi\epsilon_g\|\phi\|^2_{W_s}\geq 0,\quad \forall(\phi,\psi)\in W_\Lambda\times W_\Lambda.$$

Thus, c_{ss} is positive semi-definite.

□

Theorem 1. *There exists a unique solution $((\mathbf{D}_s,\Phi_\Lambda),(\Phi_s,\xi))\in(V_s\times W_\Lambda)\times W_s\times H^{1/2}(\partial\Omega_N)$ to problem* (4.5)*.*

Proof. Since the right-hand side of the equation is continuous in L^2, a, b_1, b_2 and c_{ss} are continuous, a is coercive on $\ker b$ and positive semi-definite, b_1 and b_2 satisfy the $\inf-\sup$ condition (4.11) and c is positive semi-definite and symmetric, the problem admits a unique solution (see [10]). □

5. 3D-1D problem on bifurcations. In the previous sections we have derived the one-dimensional formulation of the electrostatic problem on a cylindrical gas domain, geometrically reduced to a straight line. In the case of electrical treeing, the defect has a much more complicated structure, possibly forked in some points. We can assume that each branch is very thin, as in Assumption 1, and extend Assumptions 2, 3 and 4 to each of them. As before, each branch is thus representable as a straight cylinder and reducible to a segment. The whole domain can thus be approximated as a one-dimensional graph where the problem on each segment is described by the system of equations (3.16). In this case we need to impose additional conditions at the graph nodes, accounting for 3D volumes at the intersection on branches and deriving reduced conditions.

Let us start by integrating the governing equation (2.5a) of the 3D problem in the gas, in primal form, over these subdomains, that we will denote by $\mathcal{J}$, and apply the divergence theorem:

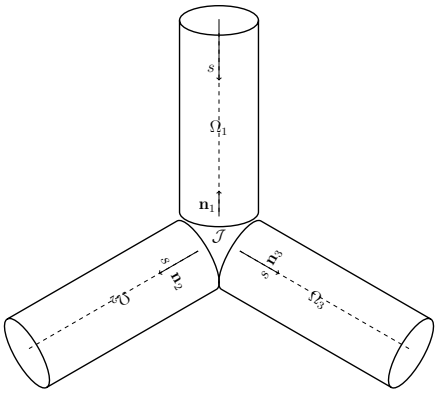

Figure 2. Junction among three cylinders Ω_1, Ω_2 and Ω_3. The boundary of the junction volume $\mathcal{J}$ is the union of the bases of the three cylinders and the lateral surface of the 3D domain.

$$\int_{\mathcal{J}} (-\nabla \cdot (\epsilon_g \nabla \Phi_g)) = -\int_{\partial \mathcal{J}} \epsilon_g \nabla \Phi_g \cdot \mathbf{n}.$$

The boundary of the junction $\mathcal{J}$ is given by the union of the bases of three cylinders $\Omega_i,\ i = 1, 2, 3$, representing the branches connected by it, and a small portion of lateral surface that we denote by $\mathcal{S}$: $\partial\mathcal{J} = (\mathcal{J} \cap \Omega_1) \cup (\mathcal{J} \cap \Omega_2) \cup (\mathcal{J} \cap \Omega_3) \cup \mathcal{S}$, as in Figure 2. We call $\mathbf{n}_i$ the unit vector with direction parallel to the axis of each cylinder Ω_i, pointing outwards from $\mathcal{J}$. If $\mathbf{n}_i$ has the same direction as $\mathbf{s}$ along the centerline Λ_i of Ω_i, we say that Λ_i becomes an *incoming edge* for the graph, with respect to the considered intersection node, otherwise it is an *outgoing edge*. In the reduction to 1D, the volume $\mathcal{J}$ is collapsed into a point connected to more than two edges, called *bifurcation node*. For each bifurcation node v_j, $j = 1, \ldots, \mathcal{N}_{\text{bif}}$, where $\mathcal{N}_{\text{bif}}$ is the number of bifurcations, we denote by $\mathcal{E}_j^+$ and $\mathcal{E}_j^-$ the sets of its incoming and outgoing edges, respectively. In the example represented by Figure 2, the vectors $\mathbf{n}_i$, $i = 1, 2, 3$, are orthogonal to the bases of cylinders forming the surface of $\mathcal{J}$, with the same direction and $\mathbf{s}$ in Ω_2 and Ω_3 and opposite direction to $\mathbf{s}$ in Ω_1. We obtain:

$$-\int_{\mathcal{J}\cap\Omega_i} \epsilon_g \nabla \Phi_g \cdot \mathbf{n} = \int_{\mathcal{J}\cap\Omega_i} \epsilon_g \nabla \Phi_g \cdot \mathbf{n}_i = \begin{cases} \displaystyle\int_{\mathcal{J}\cap\Omega_i} \epsilon_g \frac{\partial \Phi_g}{\partial s}, & i = 1, \\ \displaystyle -\int_{\mathcal{J}\cap\Omega_i} \epsilon_g \frac{\partial \Phi_g}{\partial s}, & i = 2, 3. \end{cases}$$

If we substitute the potential Φ_g with the splitting introduced in equation (3.5), we obtain:

$$\int_{\mathcal{J}\cap\Omega_i} \epsilon_g \frac{\partial \Phi_g}{\partial s} = \int_{\mathcal{J}\cap\Omega_i} \epsilon_g \frac{d\Phi_\Lambda}{ds} + \int_{\mathcal{J}\cap\Omega_i} \epsilon_g \frac{d\Phi_r}{ds}\phi.$$

Assuming that the branches can be approximated by cylinders, then the bases are circles of radius R_i and the integral becomes:

$$\int_{\mathcal{J}\cap\Omega_i} \epsilon_g \frac{d\Phi_\Lambda}{ds} + \int_{\mathcal{J}\cap\Omega_i} \epsilon_g \frac{d\Phi_r}{ds}\phi = \epsilon_g \frac{d\Phi_\Lambda}{ds}\pi R_i^2 + \epsilon_g \frac{d\Phi_r}{ds} \int_0^{2\pi}\int_0^R r^2 r dr = \pi R_i^2 \epsilon_g \frac{d\Phi_\Lambda}{ds} + \frac{\pi}{2} R_i^4 \epsilon_g \frac{d\Phi_r}{ds}.$$

Let us denote by $\Phi_{\Lambda,i}$ and $\Phi_{r,i}$ the corresponding unknowns on each branch Ω_i, $a_i = \pi R_i^2 \epsilon_g$ and $b_i = \dfrac{\pi}{2} R_i^4 \epsilon_g \dfrac{d\Phi_{r,i}}{ds}$, $i = 1, 2, 3$. Then, equation (2.5a), integrated over $\mathcal{J}$, becomes:

$$a_1 \frac{d\Phi_{\Lambda,1}}{ds} + b_1 - a_2 \frac{d\Phi_{\Lambda,2}}{ds} - b_2 - a_3 \frac{d\Phi_{\Lambda,3}}{ds} - b_3 = \int_{\mathcal{J}} f - \int_{\mathcal{S}} \epsilon_g \nabla \Phi_g \cdot \mathbf{n}.$$

The quantities b_i, dependent on R_i^4, $\int_{\mathcal{J}} f$, proportional to R_i^3, are negligible, compared to a_i. Moreover, according to the splitting (3.5) of Φ_g, the normal component $\nabla \Phi_g \cdot \mathbf{n}$ is only dependent on R_i^2. If we integrate it on $\mathcal{S}$, whose area is of order R_i^2, the term $-\int_{\mathcal{S}} \epsilon_g \nabla \Phi_g \cdot \mathbf{n}$ is of order R_i^4 and, thus, negligible. Then, the condition on the junctions in the case of an arbitrary number of edges becomes:

$$\sum_{i \in \mathcal{E}_j^+} a_i \frac{d\Phi_{\Lambda,i}}{ds} = \sum_{i \in \mathcal{E}_j^-} a_i \frac{d\Phi_{\Lambda,i}}{ds}, \quad j = 1, \dots, \mathcal{N}_{\text{bif}}.$$

The final problem reads as follows:

$$\begin{cases} \epsilon_s^{-1} \mathbf{D}_s + \nabla \Phi_s = 0, & \text{in } \Omega, \\ \nabla \cdot \mathbf{D}_s - 4\pi\epsilon_g \displaystyle\sum_{i \in \mathcal{E}} (\Phi_{\Lambda,i} - \hat{\Phi}_s) \delta_{\Lambda,i} = -2\pi \sum_{i \in \mathcal{E}} R_i g_i \delta_{\Lambda,i}, & \text{in } \Omega, \\ -\pi R_i^2 \dfrac{d}{ds} \left(\epsilon_g \dfrac{d\Phi_{\Lambda,i}}{ds} \right) + 4\pi\epsilon_g \left(\Phi_{\Lambda,i} - \hat{\Phi}_s \right) = \pi R_i^2 \dfrac{q_i}{\epsilon_0}, & \text{on } \Lambda_i,\ i = 1, \dots, \mathcal{N}_e, \\ \Phi_{\Lambda,i} = \hat{\bar{\Phi}}_g, & \text{on } \mathcal{N}_D, \\ \dfrac{d\Phi_{\Lambda,i}}{ds} = -\dfrac{2}{\epsilon_g} g, & \text{on } \mathcal{N}_N, \\ \displaystyle\sum_{i \in \mathcal{E}_j^+} a_i \frac{d\Phi_{\Lambda,i}}{ds} = \sum_{i \in \mathcal{E}_j^-} a_i \frac{d\Phi_{\Lambda,i}}{ds}, & \text{on } \mathcal{N}_{\text{bif}},\ j = 1, \dots, \mathcal{N}_{\text{bif}}, \\ \Phi_s = \bar{\Phi}_s, & \text{on } \partial\Omega_D, \\ \mathbf{D}_s \cdot \mathbf{n} = \nu, & \text{on } \partial\Omega_N, \end{cases} \tag{5.1}$$

where we have denoted by $\mathcal{N}_e$ the number of edges of the one-dimensional graph, $\mathcal{N}_N$ the set of nodes of Λ where Neumann conditions are imposed, $\mathcal{N}_D$ the set of Dirichlet nodes of Λ and $\mathcal{N}_{\text{bif}}$ the number of bifurcation nodes.

6. Numerical methods. We present a discretization based on Finite Element Methods (FEM) for the numerical solution of problem (5.1). We employ independent meshes for the one and three-dimensional domains, consisting of segments and tetrahedra, respectively. In particular, in presence of bifurcations, the one-dimensional domain can be seen as a quantum graph, i.e. a graph endowed with an implicit metric structure an a differential operator defined on its edges and vertices (see [6] for details). Arioli and Benzi [2] proposed an extension of FEM on such domains, where a partition of each edge is obtained by the addition of further nodes, thus creating a structure called *extended graph*. The three-dimensional domain Ω, instead, is partitioned in a tetrahedral conforming mesh on which we apply mixed FEM [8].

The weak formulation for the complete problem (5.1) reads as follows:

Find $(\mathbf{D}_s,\ \Phi_s,\ \Phi_\Lambda,\ \lambda_N,\ \lambda_D) \in V_s \times W_s \times W_\Lambda \times H^{-1/2}(\partial\Omega_N) \times \mathbb{R}$ such that:

$$\begin{cases} \mathcal{A}(\mathbf{D}_s, \mathbf{v}) + \mathcal{B}(\mathbf{v}, \Phi_s) = \mathcal{F}_D(\mathbf{v}), & \forall \mathbf{v} \in V_s, \\ \mathcal{B}(\mathbf{D}_s, \phi) + c(\Phi_\Lambda - \hat{\Phi}_s, \hat{\phi}) + l(\lambda_N, \mathbf{v}) = \mathcal{G}(\hat{\phi}), & \forall \phi \in W_s, \\ \mathcal{A}_\Lambda(\Phi_\Lambda, \psi) + c(\Phi_\Lambda - \hat{\Phi}_s, \psi) + d(\lambda_D, \psi) = \mathcal{F}(\psi), & \forall \psi \in W_\Lambda, \\ l(\xi_N, \mathbf{D}_s) = \mathcal{F}_N(\xi_N), & \forall \xi_N \in H^{-1/2}(\partial\Omega_N), \\ d(\xi_D, \Phi_\Lambda) = \mathcal{F}_{D,\Lambda}(\xi_D), & \forall \xi_D \in \mathbb{R} \end{cases}$$

where we have defined

$$\begin{aligned} l: \quad & V_s \times H^{-1/2}(\partial\Omega_N) \longrightarrow \mathbb{R}, \qquad l(\nu, \mathbf{v}) = \int_{\partial\Omega_N} \nu \mathbf{v} \cdot \mathbf{n}; \\ d: \quad & W_s \times \mathbb{R} \longrightarrow \mathbb{R}, \qquad d(\nu, \psi) = \nu(0)\psi; \\ \mathcal{F}_D: \quad & V_s \longrightarrow \mathbb{R}, \qquad \mathcal{F}_D(\mathbf{v}) = -\int_{\partial\Omega_D} \bar{\Phi}_s \mathbf{v} \cdot \mathbf{n}; \\ \mathcal{G}: \quad & W_s \longrightarrow \mathbb{R}, \qquad \mathcal{G}(\phi) = < G, \phi >; \\ \mathcal{F}: \quad & W_\Lambda \longrightarrow \mathbb{R}, \qquad \mathcal{F}(\psi) = < F, \psi > \\ \mathcal{F}_N: \quad & H^{-1/2}(\partial\Omega_N) \longrightarrow \mathbb{R}, \qquad \mathcal{F}_N(\nu) = \int_{\partial\Omega_N} \nu \bar{\mu}; \\ \mathcal{F}_{D,\Lambda}: \quad & \mathbb{R} \longrightarrow \mathbb{R}, \qquad \mathcal{F}_{D,\Lambda}(\nu) = \hat{\bar{\Phi}}_g \nu, \end{aligned}$$

while $\mathcal{A}$, $\mathcal{B}$, c, $\mathcal{A}_\Lambda$, F, G and all the aforementioned spaces were introduced in Section 4.
Here we have imposed the Neumann boundary conditions on the 3D domain and Dirichlet ones on the 1D by means of Lagrange multipliers λ_N and λ_D. Notice that the conditions at the bifurcations are natural for the primal formulation of the 1D problem.

6.1. DISCRETE WEAK FORMULATION. For the discretization of the one-dimensional problem on Λ (see [5]) we start by introducing a set of $n_e + 1$ equispaced points x_j^e, $j = 0, 1, \ldots, n_e$, on each edge e, partitioning it into n_e intervals of length k_e, and associate to each internal point $x_j^e,\ j = 1, \ldots, n_e - 1$ the standard hat basis function ψ_j^e. We also introduce the functions $\phi_v,\ v \in \mathcal{N}$, such that $\phi_v = 1$ on the vertex v, $\phi_v = 0$ on all the other nodes on the neighboring edges of v and is piecewise linear on each segment of the mesh. This set of functions forms a basis for the discrete space of piece-wise polynomial functions of order 1 on the neighboring segments to each bifurcation node.

Then, we define the FEM space on Λ as the direct sum of spaces spanned by all the sets of basis functions $\psi_j^e,\ e \in \mathcal{E}$ and $\phi_v,\ v \in \mathcal{N}$:

$$W_{\Lambda,k} = \left(\bigoplus_{e \in \mathcal{E}} W_{\Lambda,k}^e \right) \oplus \text{span}\{\phi_v\}_{v \in \mathcal{N}},$$

where $W_{\Lambda,k}^e = \left\{ w \in W_\Lambda \ :\ w\big|_{[x_j^e, x_{j+1}^e]} \in \mathbb{P}^1,\ j = 0, 1, \ldots, n_e - 1 \right\}$ denotes the finite-dimensional space of piecewise linear functions on the edge e.

Finally, let us denote by $\{\psi_i\}_{i=1}^{\dim(W_{\Lambda,k})}$ the set of all the basis functions of $W_{\Lambda,k}$, whose linear combinations characterize all the elements in this finite-dimensional space:

$$v = \sum_{i=1}^{\dim(W_{\Lambda,k})} v_i \psi_i, \quad \forall v \in W_{\Lambda,k}.$$

In particular, it holds for our discrete approximation of the unknown Φ_Λ, whose expansion coefficients we denote by $\mathbf{\Phi_{\Lambda,k}} \in \mathbb{R}^{n_\Lambda}$, with $n_\Lambda = \dim(W_{\Lambda,k})$.

For the three-dimensional problem we employ the standard Raviart-Thomas dual mixed FEM spaces of lowest order on a tetrahedral mesh $\mathcal{T}_h = \{T\}$ made of n_T elements, discussed in [3]. The considered finite-dimensional subspaces of V_s, W_s and $H^{-1/2}(\partial\Omega_N)$ are, respectively:

$$\begin{aligned} V_{s,h} &= \left\{ \mathbf{v} \in V_s \ : \ \mathbf{v}\big|_T \in \mathbb{RT}^0(T) \ \forall T \in \mathcal{T}_h \right\}, \\ W_{s,h} &= \left\{ \phi \in W_s \ : \ \phi\big|_T \in \mathbb{P}^0(T) \ \forall T \in \mathcal{T}_h \right\}, \\ H_h^{-1/2} &= \left\{ \nu \in W_s \ : \ \nu\big|_{\Gamma_j} \in \mathbb{P}^0(\Gamma_j), \ j = 1, \dots, n_\Gamma \right\}, \end{aligned}$$

where $\{\Gamma_j\}_{j=1}^{n_\Gamma}$ is the partition of $\partial\Omega_N$ induced by the 3D mesh $\mathcal{T}_h$, $\mathbb{RT}^0$ is the Raviart-Thomas (RT) of lowest degree [32] and $\mathbb{P}^0$ the space of polynomials of order 0. Then, $\dim(V_{s,h}) = n_F$, $\dim(W_{s,h}) = n_T$ and $\dim(H_h^{-1/2}) = n_\Gamma$, where n_F, n_T and n_Γ are the number of faces, elements of 3D mesh $\mathcal{T}_h$ and elements of the partition $\{\Gamma_j\}_{j=1}^{n_\Gamma}$ of the boundary, respectively.
Let $\{\mathbf{v}_i\}_{i=1}^{n_F}$, $\{\phi_i\}_{i=1}^{n_T}$ and $\{\nu_i\}_{i=1}^{n_\Gamma}$ be the bases of the spaces $V_{s,h}$, $W_{s,h}$ and $H_h^{-1/2}$, respectively, and denote by $\mathbf{D}_{s,h}$, $\mathbf{\Phi}_{s,h}$ and $\boldsymbol{\lambda}_{N,h}$ the vectors of expansion coefficients of the discrete approximations of $\mathbf{D}_s$, Φ_s and λ_N with respect to these bases. Then, the discrete weak formulation with Lagrange multipliers of the mixed-dimensional problem (5.1) is the following:

Find $(\mathbf{D}_{s,h},\ \mathbf{\Phi}_{s,h},\ \Phi_{\Lambda,k},\ \boldsymbol{\lambda}_{N,h},\ \lambda_D) \in \mathbb{R}^{n_T} \times \mathbb{R}^{n_T} \times \mathbb{R}^{n_\Lambda} \times \mathbb{R}^{n_\Gamma} \times \mathbb{R}$ such that:

$$\begin{cases} \mathcal{A}(\mathbf{D}_{s,h}, \mathbf{v}_h) + \mathcal{B}(\mathbf{v}_h, \mathbf{\Phi}_{s,h}) = \mathcal{F}_D(\mathbf{v}_h), & \forall \mathbf{v}_h \in \mathbb{R}^{n_T}, \\ \mathcal{B}(\mathbf{D}_{s,h}, \boldsymbol{\phi}_h) + c_{\Lambda s}(\mathbf{\Phi}_{\Lambda,k}, \hat{\boldsymbol{\phi}}_h) - c_{ss}(\hat{\mathbf{\Phi}}_{s,h}, \hat{\boldsymbol{\phi}}_h) + l(\boldsymbol{\lambda}_{N,h}, \mathbf{v}_h) = \mathcal{G}(\hat{\boldsymbol{\phi}}_h), & \forall \boldsymbol{\phi}_h \in \mathbb{R}^{n_T}, \\ \mathcal{A}_\Lambda(\mathbf{\Phi}_{\Lambda,k}, \boldsymbol{\psi}_k) + c_{\Lambda\Lambda}(\mathbf{\Phi}_{\Lambda,k}, \psi_k) - c_{\Lambda s}(\hat{\mathbf{\Phi}}_{s,h}, \boldsymbol{\psi}_k) + d(\lambda_D, \boldsymbol{\psi}_k) = \mathcal{F}(\boldsymbol{\psi}_k), & \forall \boldsymbol{\psi}_k \in \mathbb{R}^{n_\Lambda}, \\ l(\boldsymbol{\nu}_{N,h}, \mathbf{D}_{s,h}) = \mathcal{F}_N(\boldsymbol{\nu}_{N,h}), & \forall \boldsymbol{\nu}_{N,h} \in \mathbb{R}^{n_\Gamma}, \\ d(\nu_D, \mathbf{\Phi}_{\Lambda,k}) = \mathcal{F}_{D,\Lambda}(\nu_D), & \forall \nu_D \in \mathbb{R} \end{cases}$$

and the corresponding linear system is given by:

$$\begin{bmatrix} A_s & B^T & 0 & L^T & 0 \\ B & C_{ss} & C_{\Lambda s}^T & 0 & 0 \\ 0 & C_{\Lambda s} & A_\Lambda & 0 & L_D^T \\ L & 0 & 0 & 0 & 0 \\ 0 & 0 & L_D & 0 & 0 \end{bmatrix} \begin{bmatrix} \mathbf{D}_{s,h} \\ \mathbf{\Phi}_{s,h} \\ \mathbf{\Phi}_{\Lambda,k} \\ \boldsymbol{\lambda}_{N,h} \\ \lambda_D \end{bmatrix} = \begin{bmatrix} \mathbf{F}_D \\ \mathbf{G} \\ \mathbf{F} \\ \mathbf{F}_N \\ F_{D,\Lambda} \end{bmatrix} \tag{6.1}$$

where the the blocks of the system matrix are defined as follows:

$$
\begin{aligned}
&[A_s]_{i,j} \quad = \mathcal{A}(\mathbf{v}_i, \mathbf{v}_j), \quad i,j = 1,\dots,n_T, \qquad [B]_{i,j} = -\int_\Omega \phi_j \nabla\cdot \mathbf{u}_i, \quad i,j = 1,\dots,n_T,\\
&[C_{\Lambda s}]_{i,j} = c_{\Lambda s}(\psi_i, \phi_j), \quad i,j = 1,\dots,n_\Lambda, \qquad [C_{ss}]_{i,j} = -c_{ss}(\hat{\phi}_i, \hat{\phi}_j), \qquad i,j = 1,\dots,n_T,\\
&[L]_{i,j} \qquad = l(\nu_i, \mathbf{v}_j), \quad \begin{matrix} i = 1,\dots,n_\Gamma, \\ j = 1,\dots,n_T, \end{matrix} \qquad [\mathbf{L}_D]_i = -d(\lambda_D, \psi_i), \qquad i = 1,\dots,n_\Lambda,\\
&[A_\Lambda]_{i,j} = -\mathcal{A}_\Lambda(\psi_i, \psi_j) - c_{\Lambda\Lambda}(\psi_i, \psi_j), \quad i,j = 1,\dots,n_\Lambda.
\end{aligned}
$$

This system is symmetric and the blocks on the first row arise from the standard mixed FEM discretization of the 3D problem (2.4a)- (2.4f) in the dielectric domain, while the coupling terms between the two domains, given by the operators $c_{\Lambda\Lambda},\ c_{ss}$ and $c_{\Lambda s}$ appear inside the block $\begin{bmatrix} C_{ss} & C_{\Lambda s}^T \\ C_{\Lambda s} & A_\Lambda \end{bmatrix}$.

6.2. NUMERICAL SOLVER. We solve the discrete linear system (6.1) iteratively with GMRES [33], and tackle the issue of possible bad conditioning of the matrix and presence of zero blocks on the diagonal using a suitable a preconditioner P.

We exploit a preconditioner discussed in Benzi *et al.* [5] for saddle-point problems of type

$$
\begin{bmatrix} M_1 & M_2^T \\ M_2 & M_3 \end{bmatrix},
$$

where M_1 is positive definite, M_2 has maximum column rank and M_3 is negative semi-definite:

$$
P = \begin{bmatrix} M_1 & 0 \\ 0 & -(M_3 - M_2 M_1^{-1} M_2^T) \end{bmatrix}^{-1}.
$$

If we apply this to our problem, where

$$
M_1 = A_s,\ M_2 = [B,\ 0,\ L,\ 0]^T \text{ and } M_3 = \begin{bmatrix} C_{ss} & C_{\Lambda s}^T & 0 & 0 \\ C_{\Lambda s} & A_\Lambda & 0 & L_D^T \\ 0 & 0 & 0 & 0 \\ 0 & L_D & 0 & 0 \end{bmatrix},
$$

we obtain:

$$
P = \begin{bmatrix} A_s & 0 & 0 \\ 0 & -\Sigma & -E^T \\ 0 & -E & 0 \end{bmatrix}^{-1},
$$

where the blocks Σ and E are defined as:

$$
\Sigma = \begin{bmatrix} C_{ss} - BA_s^{-1}B^T & C_{\Lambda s}^T & -BA_s^{-1}L^T \\ C_{\Lambda s} & A_\Lambda & 0 \\ -LA_s^{-1}B^T & 0 & -LA_s^{-1}L^T \end{bmatrix}, \qquad E = \begin{bmatrix} 0 & L_D & 0 \end{bmatrix}.
$$

Since the inverse of a diagonal block matrix is a diagonal block matrix with diagonal blocks given by the inverse of the original diagonal blocks, we need to invert the bottom-right block of the

resulting matrix, which is again possibly ill-conditioned and saddle-point. Therefore, we adopt the same strategy, thus obtaining the following block-diagonal preconditioner in the end:

$$P = \begin{bmatrix} A_s^{-1} & 0 & 0 \\ 0 & -\Sigma^{-1} & 0 \\ 0 & 0 & -E\Sigma^{-1}E^T \end{bmatrix}.$$

A deep investigation of the properties of this final preconditioner is still an ongoing work. However, as we will see in the next section, the number of iterations needed by the GMRES solver is moderate and allows the solution of the presented coupled problem in reasonable time.

7. Results. We conclude this work by presenting some tests on a simple three-dimensional cylindrical domain, coupled with different one-dimensional geometries approximating thin inclusions. In particular, in Section 7.1 we analyze a straight line going from the center of the top basis of the cylinder to the center of the bottom basis, a simple geometry that allows us to compare the numerical solution to the reduced 1D-3D problem (4.1a)- (4.1g) to that of the original 3D-3D problem (2.1). Knowing the exact solution, we can validate the model as the radius of Ω_g tends to 0 and evaluate the dependence of the accuracy on the size of the elements in the one-dimensional mesh. Then, in Section 7.2 we observe the effect of an immersed tip inside the 3D domain and in Section 7.3 we move to the solution of a very complex electrical treeing. In all the tests the domain Ω consists of a cylinder whose bases are parallel to the x, y plane and centered in $(0.5, 0.5, 0)$ and $(0.5, 0.5, 1)$, respectively, with radius $R_s = 1$. For all these tests we have considered the same dielectric constant in both domains: $\epsilon_s = \epsilon_g = 1$.

7.1. TC1: CYLINDER AND STRAIGHT LINE. We start with a simple geometry, represented in Figure 3, consisting of the cylinder introduced above, discretized with a finer mesh close to the centerline, and a line with endpoints in the centers of the bases. In particular, we consider elements with maximum radius 10^{-2} in the proximity of Λ and 10^{-1} in the rest of the domain. The one-dimensional domain is, instead, partitioned into 100 segments. We suppose that this geometry is the mixed-dimensional approximation of two three-dimensional domains where the innermost one, representing the gas, is a cylinder of given radius R. Thus, we consider the following exact solution, adapted from [21] on Ω_s and Ω_g:

$$\begin{aligned}
\Phi_s^{\text{ex}}(r,s) &= \left[1 - \log\left(\frac{r}{R}\right)\right] R, && \text{in } \Omega_s, \\
\Phi_g^{\text{ex}}(r,s) &= \frac{1}{2}\frac{r^2}{R} + \frac{1}{2}R, && \text{in } \Omega_g, \\
\mathbf{D}_s^{\text{ex}}(r,s) &= \frac{R}{r}\mathbf{r}, && \text{in } \Omega_s, \\
\mathbf{D}_g^{\text{ex}}(r,s) &= \frac{r}{R}\mathbf{r}, && \text{in } \Omega_g,
\end{aligned}$$

Notice that all the quantities only depend on the radial coordinate r and the electric fields only have non-zero radial component, the continuity condition of the potential on the interface is satisfied and the jump of the normal component of the electric field is zero. Moreover, if we decompose the gas potential Φ_g^{ex} as in equation (3.5), we obtain $\Phi_r = \Phi_\Lambda = \dfrac{1}{2R}$ on Λ.
From this exact solution we can compute the boundary conditions and forcing terms of our specific problem, obtaining:

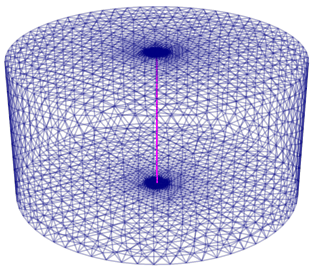

Figure 3. **TC1 -** Discretizations of the three-dimensional (blue) and one-dimensional (purple) domains.

$$
\begin{cases}
\mathbf{D}_s + \nabla \Phi_s = 0, & \text{in } \Omega, \\
\nabla \cdot \mathbf{D}_s - 4\pi(\Phi_\Lambda - \hat{\Phi}_s)\delta_\Lambda = 0, & \text{in } \Omega, \\
-\pi R^2 \dfrac{d}{ds}\left(\dfrac{d\Phi_\Lambda}{ds}\right) + 4\pi\left(\Phi_\Lambda - \hat{\Phi}_s\right) = 2\pi R, & \text{on } \Lambda, \\
\Phi_\Lambda(0) = \Phi_\Lambda(1) = \dfrac{1}{2}R, & \\
\Phi_s = \Phi_s^{\text{ex}}, & \text{on } \partial\Omega_D, \\
\mathbf{D}_s \cdot \mathbf{n} = R, & \text{on } \partial\Omega_N.
\end{cases}
\tag{7.1}
$$

Here the Neumann boundary $\partial\Omega_N$ coincides with the two bases of the cylinder and the Dirichlet boundary $\partial\Omega_D$ with its lateral surface.
In Figures 4-5 we can observe the computed potential and electric field in the three-dimensional dielectric domain. The radial decrease of the potential on the top basis, expected as a consequence of the charge distribution along the axis of the cylinder, is shown in Figure 4, is also observed in Figure 5a, with the expected value on the boundary. The major difficulty in the approximation is represented by the electric field, which presents a singularity on the centerline Λ, with magnitude going to infinity. Indeed, we can observe in Figure 4 that the arrows representing its direction and magnitude, become much larger closer to the center, and in Figure 5b its magnitude shows a rapid increase there.
These results are comparable to the numerical solution of the equidimensional original three-dimensional problem resolved by a fine grid and present qualitatively similar radial trend for the potential and direction and intensity of the electric field. For this comparison we have fixed the radius of the inner cylinder as $R = 10^{-2}$. We can observe in Figure 6 that the region where the potential has the highest values in the 3D problem is wider because it coincides with the original gas-filled cylinder, while for the mixed-dimensional solution it is concentrated along the line Λ.

Finally, knowing the exact solution, we can compute the error committed in the approximation of the electric potential in the dielectric domain, in terms of the L^2 norm on Ω, computed as error $= \|\Phi - \Phi_{ex}\|_{L^2(\Omega)}$. We want to investigate the dependence of this error on the radius R of the initial equi-dimensional coupled problem. As R decreases, tending to zero, the starting three-dimensional cylindrical gas domain Ω_g tends to collapse on the centerline Λ and we would expect the solution given by the mixed-dimensional problem to approximate better and better the exact solution to the original problem.
Figure 7 shows the plot of the L^2 error on the coarse mesh discussed above. We can see that the

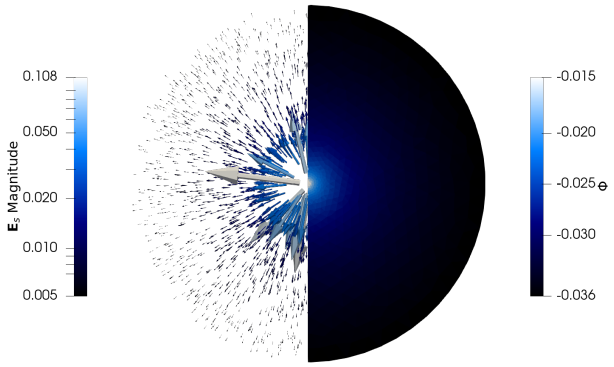

Figure 4. **TC1 -** Computed potential Φ (right half) and electric field $\mathbf{D}_s$ (left half) in the dielectric domain, osbserved from the top basis of the domain Ω.

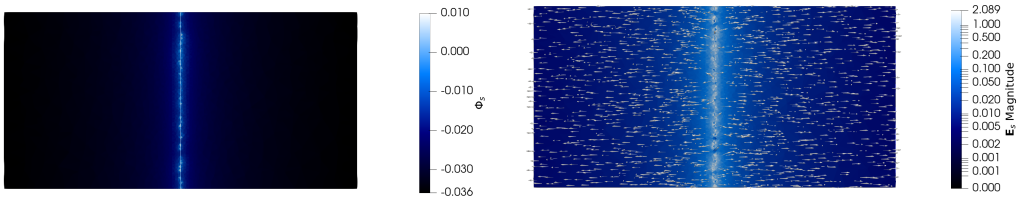

(a) Electric potential (b) Electric field

Figure 5. **TC1 -** Computed potential Φ_s and electric field $\mathbf{D}_s$ in the 3D dielectric domain on a longitudinal section of Ω. The magnitude of $\mathbf{D}_s$ is expressed in logarithmic scale and the arrows are tangential to the field streamlines.

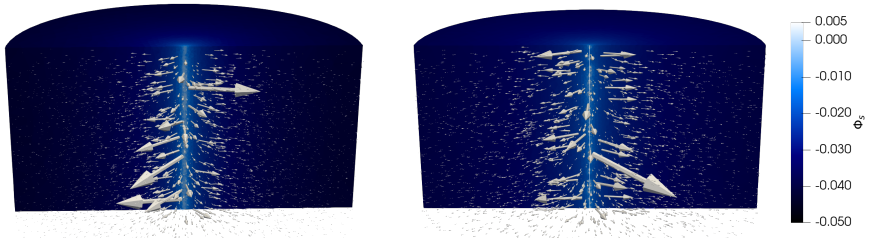

(a) 3D-3D problem (b) 3D-1D problem

Figure 6. **TC1 -** Computed potential Φ_s and electric field $\mathbf{D}_s$ in the 3D dielectric domain on a longitudinal section of Ω. Comparison between the result on the original equi-dimensional 3D problem and on the mixed-dimensional 1D-3D domain.

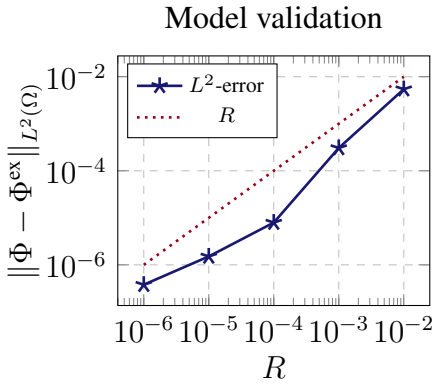

Figure 7. **TC1 -** L^2 error on the numerical approximation of the potential Φ in the dielectric domain when the radius R of the original 3D gas domain Ω_g decreases from 10^{-2} to 10^{-6}.

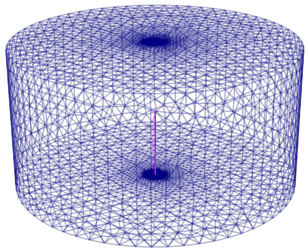

Figure 8. **TC2 -** Discretizations of the three-dimensional (blue) and one-dimensional (purple) domains.

error decreases with R, and a linear dependence is observed. This plot provides us with a validation for the proposed geometrical reduction of the model.

7.2. TC2: CYLINDER AND IMMERSED STRAIGHT LINE. As second test case we observe the solution to the problem on a mixed-dimensional domain made of a cylinder and a straight line having one end on the bottom basis and the other one inside the three-dimensional volume. On the immersed end of the 1D domain we imposed a null-flux condition for the potential Φ_Λ, and we consider the same sources and boundary data as in problem (7.1).

We can observe in Figure 9a that the potential still has a radial decrease from the charged line towards the lateral surface of the cylinder and the region where it is most intense is very close the charged line. This is due to both the geometry of the one-dimensional domain and to the boundary effect related to the Dirichlet condition on the bottom basis, as discussed in the previous section. Figure 9b represents the streamlines of the electric field and its magnitude. The magnitude presents a steep increase near the one-dimensional domain, reflecting the singularity produced by a charged line, while the streamlines have the same radial direction as in Figure 5b close to the bottom, but tend to describe hyperbolas with smaller and smaller amplitude closer to the tip, as we would expect the electric field generated by a finite charged line to be. In this Figure we can also notice the importance of a sufficient mesh refinement also in the region above the one-dimensional domain, in order to capture this behavior.

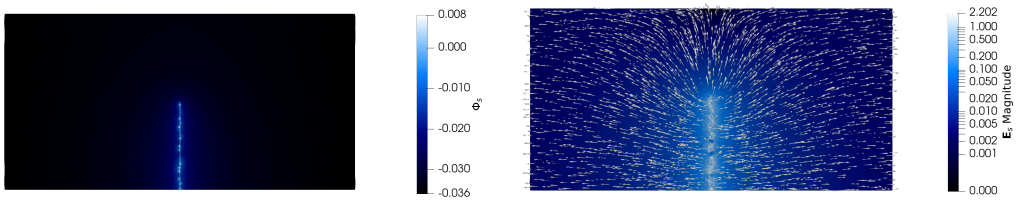

(a) Electric potential (b) Electric field

Figure 9. **TC2 -** Computed potential Φ_s and electric field $\mathbf{D}_s$ in the 3D dielectric domain on a longitudinal section of Ω. The magnitude of $\mathbf{D}_s$ is expressed in logarithmic scale and the arrows are tangential to the field streamlines.

7.3. TC3: ELECTRICAL TREEING. The final test we present is made on a ramified domain representing the reduction to a one-dimensional graph of a typical electrical treeing, immersed a cylindrical domain (see Figure 10). The discretization is based on a coarse three-dimensional grid, refined in a co-axial cylinder enclosing the treeing. For the one-dimensional discretization, we simply take as mesh segments the edges of the graph. This realistic geometry was experimentally obtained from an existing defect in an electric cable: the 3D electrical treeing was detected via X-ray computed tomography [34, 35, 36] and the 1D structure was extracted as its skeleton. It is made of 12544 segments and is coupled with a tetrahedral grid on the cylinder composed of 50859 elements.

In Figure 11a, representing a longitudinal section of the cylinder, we can observe that the potential is more intense closer to regions of the cylinder with high concentration of 1D edges, as expected. The electric field on the same section is displayed in Figure 11b, where the highest magnitude is observed in proximity of the ramification and the direction is radial with respect to segments, and curved exiting the tips, in agreement with Test Case 2.

The numerical solution on these grids was computed by a C++ parallel implementation of the solver presented in Section 6. The implementation is based on the Morgana complex modelling code [38] and relies on the Trilinos library [37]. The computational time requested for the parallel solution on six cores of a laptop with 16 GiB RAM, Intel(R) Core(TM) i5-9600K CPU, was approximately 5 minutes and 40 seconds, with 266 GMRES iterations with a tolerance 10^{-10} on the residual. A speedup could be obtained by employing a more ad hoc preconditioner, reducing the number of iterations of the solver. This is a noteworthy result, considering that such an extended defect could hardly be discretized in three-dimensions, due to its geometrical complexity, while thanks to the mixed-dimensional reduction we were able to solve the problem in reasonable time.

8. Conclusions. Starting from the coupled three-dimensional electrostatic problem in two domains with different dielectric constants, we have deduced a reduced mixed-dimensional model describing the evolution of electric field and potential on a one-dimensional domain embedded in a large three-dimensional one. This problem is relevant because, together with the drift and diffusion of charged particles in the dielectric domain, and the chemical reactions, it models the partial discharges occurring inside insulating components of electric cables, and leading to the formation of electrical trees and their eventual deterioration. We have proven the well-posedness of the resulting continuous problem and solved it numerically with Finite Elements.
We managed to conserve in the reduced problem some tricky properties of the electric field, such

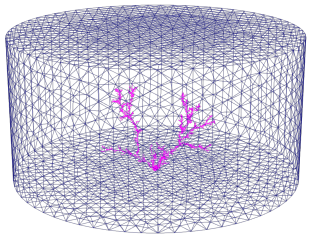

Figure 10. **TC3 -** Discretizations of the three-dimensional (blue) and one-dimensional (purple) domains.

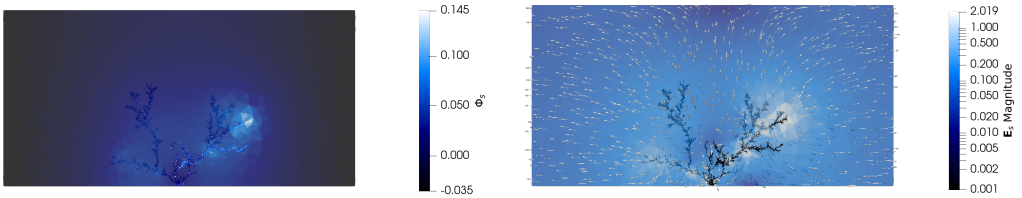

(a) Electric potential (b) Electric field

Figure 11. **TC3 -** Computed potential Φ_s and electric field $\mathbf{D}_s$ in the 3D dielectric domain on a longitudinal section of Ω. The magnitude of $\mathbf{D}_s$ is expressed in logarithmic scale and the arrows are tangential to the field streamlines.

as the jump of its normal component across the interface between the two domains, and to incorporate in a natural way the interface conditions in the coupling terms. Moreover, we only required a reasonable assumption on the concentration of charge on each section of the gas domain and derived the corresponding profile of an electric potential produced by it. This way, we are not forced to approximate the potential as constant on sections, and consequently lose information on its profile and disregard the continuity condition on the interface.

We have validated the reduced model by comparing the approximated and exact solution on a simple geometry as the radius of the original three-dimensional gas domain decreases (Section 7.1) and then qualitatively observed the solution on more complex geometries, such as an actual electrical treeing. The geometrical reduction proves crucial in more realistic cases: it allowed us to simulate this on a standard laptop in about half and hour, while the three-dimensional mesh of the defect could hardly be created.

In order to further reduce computing time future work could address the improvement of the preconditioner proposed in Section 6.2, since a more tailored one would make the GMRES require less iterations before convergence. Future work also includes the possibility to explore the Extended Finite Element Methods (XFEM) to better fit the singularity of the three-dimensional fields around the lines and a coupling with time-dependent evolution of the charge densities in the gas, requiring a model reduction as well.

References.

[1] P. F. Antonietti, L. Formaggia, A. Scotti, M. Verani, and N. Verzott, "Mimetic finite difference approximation of flows in fractured porous media," *ESAIM: Mathematical Modelling and Numerical Analysis*, vol. 50, no. 3, pp. 809–832, 2016.

[2] M. Arioli and M. Benzi, "A finite element method for quantum graphs," *IMA Journal of Numerical Analysis*, vol. 38, no. 3, pp. 1119–1163, 2018.

[3] I. Babuška and G. N. Gatica, "On the mixed finite element method with lagrange multipliers," *Numerical Methods for Partial Differential Equations: An International Journal*, vol. 19, no. 2, pp. 192–210, 2003.

[4] S Bahadoorsingh and S. Rowland, "The role of power quality in electrical treeing of epoxy resin," in *2007 Annual Report-Conference on Electrical Insulation and Dielectric Phenomena*, IEEE, 2007, pp. 221–224.

[5] M. Benzi, G. H. Golub, and J. Liesen, "Numerical solution of saddle point problems," *Acta Numerica*, vol. 14, 1–137, 2005.

[6] G. Berkolaiko and P. Kuchment, *Introduction to quantum graphs*. American Mathematical Soc., 2013.

[7] C. Bernardi, C. Canuto, and Y. Maday, "Generalized inf-sup conditions for chebyshev spectral approximation of the stokes problem," *SIAM Journal on Numerical Analysis*, vol. 25, no. 6, pp. 1237–1271, 1988.

[8] D. Boffi, F. Brezzi, M. Fortin, *et al.*, *Mixed finite element methods and applications*. Springer, 2013, vol. 44.

[9] J. Březina and P. Exner, "Extended finite element method in mixed-hybrid model of singular groundwater flow," *Mathematics and Computers in Simulation*, vol. 189, pp. 207–236, 2021.

[10] F. Brezzi, "On the existence, uniqueness and approximation of saddle-point problems arising from lagrangian multipliers," *Publications mathématiques et informatique de Rennes*, no. S4, pp. 1–26, 1974.

[11] F. Brezzi and M. Fortin, *Mixed and hybrid finite element methods*. Springer Science & Business Media, 2012, vol. 15.

[12] G. Buccella, A. Villa, D. Ceresoli, R. Schurch, L. Barbieri, R. Malgesini, and D. Palladini, "A computational modelling of carbon layer formation on treeing branches," *Modelling and Simulation in Materials Science and Engineering*, vol. 31, no. 3, p. 035 001, 2023.

[13] L. Cattaneo and P. Zunino, "A computational model of drug delivery through microcirculation to compare different tumor treatments," *International journal for numerical methods in biomedical engineering*, vol. 30, no. 11, pp. 1347–1371, 2014.

[14] D. Cerroni, F. Laurino, and P. Zunino, "Mathematical analysis, finite element approximation and numerical solvers for the interaction of 3d reservoirs with 1d wells," *GEM-International Journal on Geomathematics*, vol. 10, pp. 1–27, 2019.

[15] C. D'Angelo, "Finite element approximation of elliptic problems with dirac measure terms in weighted spaces: Applications to one-and three-dimensional coupled problems," *SIAM Journal on Numerical Analysis*, vol. 50, no. 1, pp. 194–215, 2012.

[16] C. D'angelo and A. Quarteroni, "On the coupling of 1d and 3d diffusion-reaction equations: Application to tissue perfusion problems," *Mathematical Models and Methods in Applied Sciences*, vol. 18, no. 08, pp. 1481–1504, 2008.

[17] C. D'angelo and A. Quarteroni, "On the coupling of 1d and 3d diffusion-reaction equations: Application to tissue perfusion problems," *Mathematical Models and Methods in Applied Sciences*, vol. 18, no. 08, pp. 1481–1504, 2008.

[18] L. Formaggia, A. Quarteroni, and A. Veneziani, *Cardiovascular Mathematics: Modeling and simulation of the circulatory system*. Springer Science & Business Media, 2010, vol. 1.

[19] L. Formaggia, A. Scotti, and F. Sottocasa, "Analysis of a mimetic finite difference approximation of flows in fractured porous media," *ESAIM: Mathematical Modelling and Numerical Analysis*, vol. 52, no. 2, pp. 595–630, 2018.

[20] G. N. Gatica and F.-J. Sayas, "Characterizing the inf-sup condition on product spaces," *Numerische Mathematik*, vol. 109, no. 2, pp. 209–231, 2008.

[21] I. G. Gjerde, K. Kumar, and J. M. Nordbotten, "A mixed approach to the poisson problem with line sources," *SIAM Journal on Numerical Analysis*, vol. 59, no. 2, pp. 1117–1139, 2021.

[22] I. G. Gjerde, K. Kumar, and J. M. Nordbotten, "A singularity removal method for coupled 1d–3d flow models," *Computational Geosciences*, vol. 24, pp. 443–457, 2020.

[23] I. G. Gjerde, K. Kumar, J. M. Nordbotten, and B. Wohlmuth, "Splitting method for elliptic equations with line sources," *ESAIM: Mathematical Modelling and Numerical Analysis*, vol. 53, no. 5, pp. 1715–1739, 2019.

[24] R. Gracie and J. R. Craig, "Modelling well leakage in multilayer aquifer systems using the extended finite element method," *Finite Elements in Analysis and Design*, vol. 46, no. 6, pp. 504–513, 2010.

[25] D. Grappein, S. Scialò, and F. Vicini, "Extended finite elements for 3d–1d coupled problems via a pde-constrained optimization approach," *Finite Elements in Analysis and Design*, vol. 239, p. 104 203, 2024.

[26] D. J. Griffiths, *Introduction to electrodynamics*. Cambridge University Press, 2023.

[27] M. Lesinigo, C. D'Angelo, and A. Quarteroni, "A multiscale darcy–brinkman model for fluid flow in fractured porous media," *Numerische Mathematik*, vol. 117, pp. 717–752, 2011.

[28] V. Martin, J. Jaffré, and J. E. Roberts, "Modeling fractures and barriers as interfaces for flow in porous media," *SIAM Journal on Scientific Computing*, vol. 26, no. 5, pp. 1667–1691, 2005.

[29] R. A. Nicolaides, "Existence, uniqueness and approximation for generalized saddle point problems," *SIAM Journal on Numerical Analysis*, vol. 19, no. 2, pp. 349–357, 1982.

[30] D. Notaro, L. Cattaneo, L. Formaggia, A. Scotti, and P. Zunino, "A mixed finite element method for modeling the fluid exchange between microcirculation and tissue interstitium," *Advances in discretization methods: discontinuities, virtual elements, fictitious domain methods*, pp. 3–25, 2016.

[31] "On the coupling of 3d and 1d navier–stokes equations for flow problems in compliant vessels," *Computer methods in applied mechanics and engineering*, vol. 191, no. 6-7, pp. 561–582, 2001.

[32] P. Raviart and J. Thomas, *A mixed finite element method for second order elliptic equations, mathematical aspects of finite element methods (i. galligani and e. magenes, eds.)* 1977.

[33] Y. Saad and M. H. Schultz, "Gmres: A generalized minimal residual algorithm for solving nonsymmetric linear systems," *SIAM Journal on scientific and statistical computing*, vol. 7, no. 3, pp. 856–869, 1986.

[34] R. Schurch, J. Ardila-Rey, J. Montana, A. Angulo, S. M. Rowland, I. Iddrissu, and R. S. Bradley, "3d characterization of electrical tree structures," *IEEE Transactions on Dielectrics and Electrical Insulation*, vol. 26, no. 1, pp. 220–228, 2019.

[35] R. Schurch, S. M. Rowland, R. S. Bradley, and P. J. Withers, "Comparison and combination of imaging techniques for three dimensional analysis of electrical trees," *IEEE Transactions on Dielectrics and Electrical Insulation*, vol. 22, no. 2, pp. 709–719, 2015.

[36] R. Schurch, S. M. Rowland, R. S. Bradley, and P. J. Withers, "Imaging and analysis techniques for electrical trees using x-ray computed tomography," *IEEE Transactions on Dielectrics and Electrical Insulation*, vol. 21, no. 1, pp. 53–63, 2014.

[37] T. Trilinos Project Team, *The Trilinos Project Website*, 2020 (acccessed May 22, 2020). [Online]. Available: https://trilinos.github.io.

[38] A. Villa, *Morgana complex modelling code*, https://www.citedrive.com/overleaf, 2019 (accessed Aug 21, 2024).

[39] A. Villa, L. Barbieri, M. Gondola, A. R. Leon-Garzon, and R. Malgesini, "A PDE-based partial discharge simulator," *Journal of Computational Physics*, vol. 345, pp. 687–705, 2017.

[40] A. Villa, L. Barbieri, R. Malgesini, and G. Buccella, "Discretization of poisson's equation in two domains with non algebraic interface conditions for plasma simulations," *Applied Mathematics and Computation*, vol. 403, p. 126 179, 2021.

MOX Technical Reports, last issues

Dipartimento di Matematica
Politecnico di Milano, Via Bonardi 9 - 20133 Milano (Italy)

73/2024 Liverotti, L.; Ferro, N.; Soli, L.; Matteucci, M.; Perotto, S.
Using SAR Data as an Effective Surrogate for Optical Data in Nitrogen Variable Rate Applications: a Winter Wheat Case Study

72/2024 Patanè, G.; Bortolotti, T.; Yordanov, V.; Biagi, L. G. A.; Brovelli, M. A.; Truong, A. Q; Vantini, S.
An interpretable and transferable model for shallow landslides detachment combining spatial Poisson point processes and generalized additive models

71/2024 Zhang, L.; Pagani, S.; Zhang, J.; Regazzoni, F.
Shape-informed surrogate models based on signed distance function domain encoding

70/2024 Panzeri, L.; Fumagalli, A.; Longoni, L.; Papini, M.; Diego, A.
Sensitivity analysis with a 3D mixed-dimensional code for DC geoelectrical investigations of landfills: synthetic tests

68/2024 Gambarini, M.; Ciaramella, G.; Miglio, E.
A gradient flow approach for combined layout-control design of wave energy parks

69/2024 Galliani, G.; Secchi, P.; Ieva, F.
Estimation of dynamic Origin–Destination matrices in a railway transportation network integrating ticket sales and passenger count data

Galliani, G.; Secchi, P.; Ieva, F.
Estimation of dynamic Origin–Destination matrices in a railway transportation network integrating ticket sales and passenger count

65/2024 Possenti, L.; Vitullo, P.; Cicchetti, A.; Zunino, P.; Rancati, T.
Modeling Hypoxia Induced Radiation Resistance and the Impact of Radiation Sources

64/2024 Cavazzutti, M.; Arnone, E.; Ferraccioli, F.; Galimberti, C.; Finos, L.; Sangalli, L.M.
Sign-Flip inference for spatial regression with differential regularization

63/2024 Vitullo, P.; Franco, N.R.; Zunino, P.
Deep learning enhanced cost-aware multi-fidelity uncertainty quantification of a computational model for radiotherapy